

*[Handwritten signature]* 12

AD A 0 4 5 3 1 4

# STUDY TO IMPROVE TURBINE ENGINE ROTOR BLADE CONTAINMENT

**K.F. Heermann  
K.R. McClure  
R.H. Eriksson**



**AUGUST 1977  
FINAL REPORT**

DDC  
**RECEIVED**  
OCT 17 1977  
*[Handwritten initials]*  
B

Document is available to the U.S. public through  
the National Technical Information Service,  
Springfield, Virginia 22161.

AD No. \_\_\_\_\_  
DDC FILE COPY.

Prepared for  
**U.S. DEPARTMENT OF TRANSPORTATION  
FEDERAL AVIATION ADMINISTRATION  
Systems Research & Development Service  
Washington, D.C. 20590**

NOTICE

This document is disseminated under the sponsorship of the Department of Transportation in the interest of information exchange. The United States Government assumes no liability for its contents or use thereof.

<p>1. Report No.  <span style="border: 1px solid black; border-radius: 50%; padding: 2px;">18</span> <span style="border: 1px solid black; border-radius: 50%; padding: 2px;">19</span>                  FAA-RD-77-199 ✓</p>	<p>2. Government Accession No.</p>	<p>3. Recipient's Catalog No.</p>	
<p>4. Title and Subtitle  <span style="border: 1px solid black; border-radius: 50%; padding: 2px;">6</span> Study to Improve Turbine Engine Rotor Blade Containment.</p>		<p>5. Report Date  <span style="border: 1px solid black; border-radius: 50%; padding: 2px;">11</span> August 1977 ✓</p>	<p>6. Performing Organization Code</p>
<p>7. Author(s)  <span style="border: 1px solid black; border-radius: 50%; padding: 2px;">10</span> K. F./Heermann, R. H./Eriksson                  K. R./McClure</p>	<p>8. Performing Organization Report No.  <span style="border: 1px solid black; border-radius: 50%; padding: 2px;">14</span> PWA-5551 ✓</p>	<p>9. Performing Organization Name and Address                  UNITED TECHNOLOGIES CORPORATION                  Pratt &amp; Whitney Aircraft Group                  Commercial Products Division                  East Hartford, Conn., 06108</p>	
<p>12. Sponsoring Agency Name and Address                  Federal Aviation Administration                  Systems Research and                  Development Service                  Washington, D. C. 20590</p>	<p>10. Work Unit No. (TRAI5)</p>	<p>11. Contract or Grant No.                  DOT-FATQWA-3857 ✓</p>	<p>13. Type of Report and Period Covered                  Final Report,                  August 1976 to August 1977,</p>
<p>15. Supplementary Notes</p>	<p>12. 55p. <span style="border: 1px solid black; border-radius: 50%; padding: 2px;">9</span></p>	<p>14. Sponsoring Agency Code                  ARD-520</p>	
<p>16. Abstract</p> <p>An engineering study on a large turbofan engine was conducted to: (1) accurately estimate the engine weight increase and design criteria necessary to contain equivalent disk fragments resulting from a rotor failure, (2) evaluate forward containment for tip fragments of fan blades, (3) identify critical structural components and loads for the loss of an equivalent fan disk fragment through analysis of the rotor/frame transient dynamic response. The fragments studied for engine containment were disk fragments with energy equivalent to two adjacent blades and an included disk serration, and four adjacent blades and three included disk serrations. The forward containment study was made to determine the additional weight required to contain or deflect turbofan engine fan blade tip fragments up to 30 degrees forward of the plane of rotation, as measured from the axis of rotation.</p> <p>The results of this study indicated significant weight increases for the engine in order to contain the equivalent disk fragments of two blades with an included disk serration and four blades with three included disk serrations. The total resultant engine weight increase (shown in Table 9) for the two blade fragment is 367 pounds and for the four blade fragment is 682 pounds.</p> <div style="text-align: right; margin-top: 20px;"> <p style="font-size: 2em; margin: 0;">D D C</p> <p style="font-size: 3em; margin: 0;">RECEIVED</p> <p style="font-size: 1.2em; margin: 0;">OCT 17 1977</p> <p style="font-size: 2em; margin: 0;">RECEIVED</p> <p style="font-size: 1.5em; margin: 0;">B</p> </div>			
<p>17. Key Words                  Turbofan engine, containment, disk fragment, blade fragment, transient dynamic response</p>	<p>18. Distribution Statement                  Document is available to the U.S. public through the National Technical Information Service, Springfield, Virginia 22161.</p>		
<p>19. Security Classif. (of this report)                  Unclassified</p>	<p>20. Security Classif. (of this page)                  Unclassified</p>	<p>21. No. of Pages                  57</p>	<p>22. Price</p>

410 116

LB

# METRIC CONVERSION FACTORS

## Approximate Conversions to Metric Measures

Symbol	When You Know	Multiply by	To Find	Symbol
<b>LENGTH</b>				
in	inches	2.5	Centimeters	cm
ft	feet	30	Centimeters	cm
yd	yards	0.9	meters	m
mi	miles	1.6	Kilometers	km
<b>AREA</b>				
in <sup>2</sup>	square inches	6.5	square centimeters	cm <sup>2</sup>
ft <sup>2</sup>	square feet	0.09	square meters	m <sup>2</sup>
yd <sup>2</sup>	square yards	0.8	square meters	m <sup>2</sup>
mi <sup>2</sup>	square miles	2.6	square kilometers	km <sup>2</sup>
ac	acres	0.4	Hectares	ha
<b>MASS (weight)</b>				
oz	ounces	28	grams	g
lb	pounds (short tons (2000 lb))	0.45 0.9	Kilograms tonnes	kg t
<b>VOLUME</b>				
fl oz	fluid ounces	30	milliliters	ml
cup	Cups	0.24	liters	l
pt	pints	0.47	liters	l
qt	quarts	0.96	liters	l
gal	gallons	3.8	liters	l
ft <sup>3</sup>	cubic feet	0.03	cubic meters	m <sup>3</sup>
yd <sup>3</sup>	cubic yards	0.76	cubic meters	m <sup>3</sup>
<b>TEMPERATURE (exact)</b>				
°F	Fahrenheit temperature	5/9 (then subtracting 32)	Celsius temperature	°C

\*1 in = 2.54 exactly. For other exact conversions and metric data, see NBS Monograph 43, U.S. Customary Units of Length and Mass, NBS-GCR-75-310, 1975.

Symbol	When You Know	Multiply by	To Find	Symbol
<b>LENGTH</b>				
mm	millimeters	0.04	inches	in
cm	centimeters	0.4	inches	in
m	meters	3.3	feet	ft
km	kilometers	1.1	yards	yd
		0.6	miles	mi
<b>AREA</b>				
cm <sup>2</sup>	square centimeters	0.16	square inches	in <sup>2</sup>
m <sup>2</sup>	square meters	1.2	square yards	yd <sup>2</sup>
km <sup>2</sup>	square kilometers	0.4	square miles	mi <sup>2</sup>
ha	hectares (10,000 m <sup>2</sup> )	2.5	acres	ac
<b>MASS (weight)</b>				
g	grams	0.035	ounces	oz
kg	kilograms	2.2	pounds	lb
t	tonnes (1,000 kg)	1.1	short tons	st
<b>VOLUME</b>				
ml	milliliters	0.03	fluid ounces	fl oz
l	liters	2.1	pints	pt
l	liters	1.06	quarts	qt
l	liters	0.26	gallons	gal
m <sup>3</sup>	cubic meters	35	cubic feet	ft <sup>3</sup>
m <sup>3</sup>	cubic meters	1.3	cubic yards	yd <sup>3</sup>
<b>TEMPERATURE (exact)</b>				
°C	Celsius temperature	9/5 (then add 32)	Fahrenheit temperature	°F



## PREFACE

This final Report describes the work conducted during the period 17 August 1976 to August 1977 by Pratt & Whitney Aircraft, East Hartford, Connecticut, under FAA Contract DOT-FATQWA-3857, for the Systems Research and Development Service of the Federal Aviation Administration. This report presents the results obtained from analytical studies aimed at improving rotor blade containment.

Mr. Karl F. Heermann served as Program Manager for Pratt & Whitney Aircraft and provided technical direction throughout the program. Mr. Kenneth R. McClure conducted the engine containment and forward containment analyses, and Mr. Richard H. Eriksson performed the rotor/frame transient dynamic response analysis. Acknowledgements are given to Commander J. J. Shea, FAA Program Manager for his participation in guiding and monitoring the performance of the program.

This report submitted on August 26, 1977 is in compliance with the report requirements of the contract schedule and was prepared under the Contractor's reference no. PWA 5551.

ACCESSION for	
NTIS	VIC Section <input checked="" type="checkbox"/>
DDC	PIC Section <input type="checkbox"/>
UNANNOUNCED	<input type="checkbox"/>
JUS	
BY	
DISTING	IDENTITY CODES
Di.	SPECIAL
A	

THIS PAGE INTENTIONALLY LEFT BLANK

## TABLE OF CONTENTS

<b>Section</b>	<b>Page</b>
1.0 Introduction	i
2.0 Study Description	3
2.1 Containment	3
2.1.1 Fragment Description	3
2.1.2 Analysis	3
2.2 Engine Dynamic Response	4
3.0 Containment Analysis	5
3.1 Engine Containment	5
3.1.1 Description of Fragment	5
3.1.2 Analytical Procedure for Fan Section	5
3.1.3 Analytical Procedure for Compressor and Turbine Section	10
3.1.4 Kinetic Energy Levels for the Disk and Blade Fragments	13
3.1.5 Engine Case Materials and Maximum Operating Temperatures	15
3.1.6 Additional Weight for Containment of Disk Fragment With Energy Equivalent to Two Adjacent Blades and an Included Disk Serration	16
3.1.7 Additional Weight for Containment of Disk Fragment With Energy Equivalent to Four Adjacent Blades and Three Included Disk Serrations	18
3.1.8 Additional Weight for Low Pressure Compressor Section With Alternate Engine Case Materials	18
3.1.9 Design Considerations and Limitations	20
3.2 Forward Containment	20
3.2.1 Description of Fragment	20

## TABLE OF CONTENTS (Continued)

Section	Page
3.2.2 Analytical Procedure	22
3.2.3 Kinetic Energy of Forward Moving Fan Blade Fragments	23
3.2.4 Additional Weight for Containment	26
4.0 Transient Response Analysis	31
4.1 Analytical Procedure	31
4.1.1 Description of Analysis	31
4.1.2 Assumptions in the Analysis	32
4.1.3 Case Impact Loads	32
4.1.4 Alternate Load Paths	32
4.1.5 Deceleration Response of Engine	34
4.2 Results of Analysis	34
4.2.1 Structural Areas of Concern	34
4.2.2 Engine Component Loads	35
4.2.3 Potential Solutions for Limiting Structural Components	37
5.0 Review of Results of The National Aeronautics and Space Administration's Rotor Burst Protection Program	39
6.0 Results	41
Glossary	43
References	44



## LIST OF ILLUSTRATIONS

Figure	Title	Page
1	Noncontained Engine Disk Failure Summary - P&WA Commercial Engine Models	2
2	Fan Containment - Single Blade Failure	6
3	Fan Blade Buckling Upon Impact With the Containment Case	6
4	Fan Containment - Multiple Blade Failure	7
5	Fan Containment - Disk Fragment With Energy Equivalent to Two Adjacent Blades and an Included Disk Serration	8
6	Region of Aft Containment Required for Fan Blade Failures	9
7	Compressor and Turbine Containment - Single Blade Failure	10
8	Compressor and Turbine Containment - Disk Fragment with Energy Equivalent to Two Adjacent Blades and an Included Disk Serration	11
9	Containment Capability of Compressor and Turbine Cases	12
10	A Two Blade and an Included Disk Serration Fragment from a Typical Turbine Engine Rotor	14
11	Description of Fan Blade Tip Fragment for Forward Containment	21
12	Fan Blade Tip Fragment Trajectories and Types of Case Damage	22
13	Fan Forward Containment - Tangential Velocity vs. Radial Reingestion Location for the "Punch Out" Type Fragment	24
14	Fan Forward Containment - Kinetic Energy vs. Radial Reingestion Location for the "Punch Out" Type Fragment in the Fan Rotor Plane	24
15	Fan Forward Containment - Trajectory Velocity vs. Radial Reingestion Location for Impact at 30 Degrees Forward of the Fan Rotor Plane	25
16	Fan Forward Containment - Kinetic Energy vs. Radial Reingestion Location for Impact at 30 Degrees Forward of the Fan Rotor Plane	26
17	Fan Forward Containment - Tangential Trajectory Angle vs. Radial Reingestion Location	27

### LIST OF ILLUSTRATIONS (Continued)

Figure	Title	Page
18	Fan Forward Containment – Case Thickness for Containment vs. Radial Reingestion Location for the “Punch Out” Type Fragment at the Fan Rotor Plane	28
19	Fan Forward Containment – Axial Trajectory Angle vs. Radial Reingestion Location for Impact at 30 Degrees Forward of the Fan Rotor Plane	28
20	Fan Forward Containment – Case Thickness for Containment vs. Radial Reingestion Location for Impact at 30 Degrees Forward of the Fan Rotor Plane	29
21	Fan Forward Containment – Case Thickness for Containment vs. Forward Axial Distance	30
22	Schematic of Rotor System for Transient Response Analysis	31
23	Rotor Transient Response – Relative Phase Between Imbalance and Impact Forces	33
24	Rotor Transient Response – Alternate Load Paths Reduce Bearing Load	33
25	Rotor Transient Response – Bi-Linear Spring Used to Simulate Rub Condition	34
26	Engine Cross Section – Structural Areas of Concern With Loss of a Fan Disk Fragment	35
27	Typical Deceleration Response With Loss of a Fan Disk Fragment	36
28	Typical Engine Response to Combined Rotating Imbalance and Impact Load	37
29	Comparison of Typical Disk Fragments Tested by the NAPTC and Disk Fragments Defined for This Study	39

## LIST OF TABLES

<b>Table</b>	<b>Title</b>	<b>Page</b>
1	<b>Kinetic Energy Developed by a Disk Fragment Compared to a Single Blade Failure</b>	15
2	<b>Engine Case Materials and Maximum Operating Temperatures</b>	16
3	<b>Engine Weight Necessary to Satisfy Present Blade Containment Requirements</b>	17
4	<b>Additional Weight for Containment of a Disk Fragment With Energy Equivalent to Two Adjacent Blades and an Included Disk Serration</b>	17
5	<b>Additional Weight for Containment of a Disk Fragment With Energy Equivalent to Four Adjacent Blades and Three Included Disk Serrations</b>	19
6	<b>Additional Weight to Contain a Low Pressure Compressor Disk Fragment With Alternate Engine Case Type Materials</b>	19
7	<b>Maximum Transient Loads for the Limiting Engine Locations</b>	36
8	<b>Rotor Transient Response – Additional Weight Required for Structural Adequacy of Limiting Engine Components</b>	38
9	<b>Total Resultant Engine Weight Increase</b>	41

## LIST OF SYMBOLS

- B** = nondimensional buckling factor defined as the ratio of the fragment tangential kinetic energy after buckling has occurred to the fragment tangential kinetic energy prior to buckling
- b<sub>x</sub>** = axial projection of the blade tip (in)
- C** = a nondimensional factor which relates the effective circumferential length of case for a disk fragment to the one pitch circumferential length for a single blade
- CF** = nondimensional containment factor
- D** = nominal diameter (in)
- d** = nondimensional factor relating to the effective axial length of case
- F** = nondimensional empirical factor based on single blade failure experience
- K** = nondimensional dynamic factor
- KE** = kinetic energy (in-lbs)
- (KE)<sub>T</sub>** = tangential kinetic energy (in-lbs)
- L** = dovetail length (in)
- M** = mass (lbs-sec<sup>2</sup>/in)
- M<sub>f</sub>** = static material factor (lbs/in<sup>2</sup>)
- N<sub>1</sub>** = rotational speed of low pressure rotor (rpm)
- N<sub>2</sub>** = rotational speed of high pressure rotor (rpm)
- n** = number of blades in a rotor stage
- P** = perimeter of the "shear plug" (in)
- PE** = potential energy (in-lbs)
- T** = dovetail thickness (in)
- t** = required minimum case thickness for containment (in)
- V** = velocity at the center of gravity (in/sec)

### LIST OF SYMBOLS (Continued)

- $\beta$  = angle between the fragment axial trajectory component and a normal to the case at the point of impact (degrees)
- $\theta$  = angle between the fragment tangential trajectory component and a normal to the case at the point of impact (degrees)
- $\pi$  = 3.1415926
- $\tau_D$  = dynamic shear strength of a material (lbs/in<sup>2</sup>)
- $\phi$  = nondimensional factor relating the mass of the "shear plug" produced in the containment case to the mass of the fragment

## 1.0 INTRODUCTION

Damage to the aircraft may occur whenever a failure occurs in a rotating stage of a turbine engine. This damage, which may be critical to the aircraft, can be reduced by minimizing the number of rotor failures and by containing within the engine nacelle any fragments resulting from a rotor stage failure. To prevent rotor failures, Pratt & Whitney Aircraft continually develops new disk and blade design procedures based on engine service experience and in-house testing. Examples are the introduction of turbine flutter criteria, incorporation of disk bore fracture mechanics criteria for all new engine designs and the practice of positioning airseals closer to the outer rim of a disk so that any failures resulting from axial seal rubs will result in smaller fragments being separated from the disk.

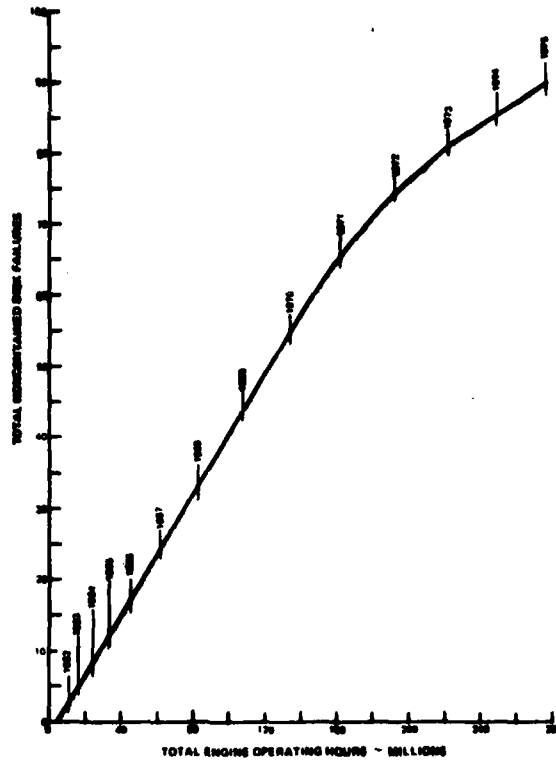
Disk failures due to material problems have been reduced by the introduction of new melting process controls, improved billet and disk ultrasonic inspection and other non-destructive inspection techniques. Material deficiencies associated with a particular heat of material are rare, however, when found, the effects of the material deficiencies are eliminated by recall of all known disks from that heat.

The results of these P&WA programs are dramatic in that the incidence of noncontained disk failures per million engine operating hours for the last three years has been a factor of two lower than the rate in the period from 1962 to 1965. This can be seen in Figure 1(a) which is a curve of noncontained disk failures versus engine operating hours and Figure 1(b) which is a curve of noncontained disk failure rate versus year.

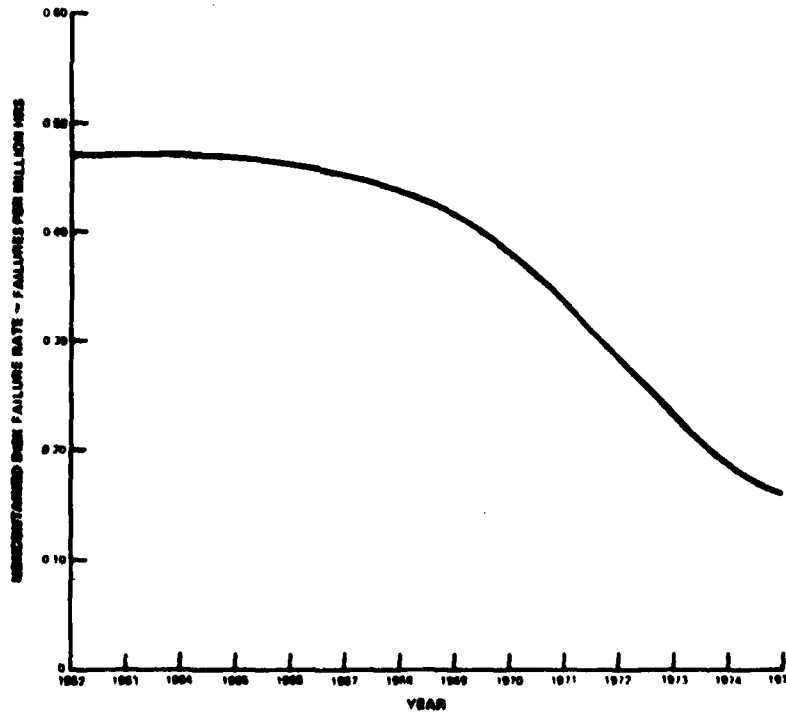
It is virtually impossible to completely eliminate disk failures. Theoretically it is desirable to contain all fragments of a failure within the engine nacelle. Historically, it has not been feasible to design an engine which would contain burst failures of an entire rotor stage because of the extremely large weight required and prohibitive performance penalties. Most disk failures though, are not as severe as a burst disk and yield fragments totaling much less than one-third of the rotor mass produced by a disk burst. The specific cases of two adjacent blades with one disk serration and four adjacent blades with three disk serrations analyzed in this study are treated as a disk failure with energy equivalent to the segments of mass specified.

P&WA engines are designed to contain blade failures within the engine cases without depending on the containment capability of the engine nacelle. They are also designed to withstand the shock of a case impact and the resulting rotor imbalance created by blade failures. In the fan section of the engine, the cases are designed to contain fan blades aft as well as in the plane of the disk. The current containment techniques with suitable modifications for multiple blades or equivalent disk fragments was used in this study to determine the additional weight needed to contain two and four blades with their included disk serrations within each section of the engine (fan, compressor and turbine).

The cases that currently provide forward fan blade containment are not a part of the engine structure. However, for this study forward containment was assumed to be provided by a case using existing case materials. In addition, a rotor/frame transient dynamic analysis of the engine response to the loss of an equivalent fan disk fragment was conducted to determine the overall engine structural integrity since typically an engine mount, case flange or bearing support failure can be as severe as the primary in plane case failure.



(A) Failures vs. Total Operating Hours



(B) Failure Rate vs. Year

Figure 1 Noncontained Engine Disk Failure Summary - P&WA Commercial Engine Models

## 2.0 STUDY DESCRIPTION

A two-part engineering study was conducted to accurately estimate the engine weight increase and design criteria necessary to contain various specified equivalent disk fragments, and identify limiting structural components and loads resulting from the loss of an equivalent fan disk fragment through analysis of a rotor/frame transient dynamic response. The study was conducted on the JT9D-59A/D-70A engine, which is compatible with any of the wide bodied aircraft in service operating at manufacturer's rated power for a standard day, maximum gross weight takeoff.

### 2.1 CONTAINMENT

The containment analysis for this study is divided into two parts: (a) concerning the engine containment and (b) concerning the forward containment analysis.

#### 2.1.1 Fragment Description

The fragments as specified in the Contract were defined as:

- (1) Disk fragments for the engine containment analysis resulting from a rotor failure with energy equivalent to:
  - (a) Two adjacent blades and their included disk serration from each disk and blade assembly of the fan unit, the low pressure compressor unit, the high pressure compressor unit, the high pressure turbine unit and the low pressure turbine unit, each broken at the outermost retention groove or member; and
  - (b) Four adjacent blades and their included disk serrations as explained above.
- (2) Fan blade tip fragments for the forward containment analysis consisting of six titanium pieces, three pieces being portions of three adjacent fan blades, measured from the leading edge of the blade to 3 inches back from the leading edge, and from the tip to 5 inches from the tip, and each being 0.2 inches thick. The other three pieces were of like size, from three adjacent fan blades 180 degrees away from the first fractures.

#### 2.1.2 Analysis

The engine containment analysis consisted of the following steps:

- (1) Determine the kinetic energy of the equivalent disk fragment at the rotor "red line" speed.
- (2) Extend the analytical procedures currently in use for blade failures to the equivalent disk fragments under study.



- (3) Determine the containment capability of the existing case structure for the equivalent disk fragment sizes under study.
- (4) Determine the additional containment capability and additional weight required to contain the equivalent disk fragment using existing engine case materials.
- (5) Determine the design criteria necessary for an additional containment capability.

Considerations of the National Aeronautics and Space Administration's Rotor Burst Protection Program were included in the engine containment section of this study.

The forward containment analysis consisted of the following steps:

- (1) Establish an analytical procedure; similar to the procedure used in the fan section, and calibrate the procedure with actual test data of simulated fan blade tip fragments.
- (2) Determine kinetic energy levels of forward moving fan blade tip fragments.
- (3) Determine the case thickness and weight required to contain or deflect the fan blade tip fragment up to 30 degrees forward of the plane of rotation.

## 2.2 ENGINE DYNAMIC RESPONSE

Utilizing the kinetic energies and forces generated for the containment analysis, a rotor/frame transient response analysis was conducted for the following equivalent disk fragments: two adjacent fan blades and their included disk serration; and four adjacent fan blades and their included disk serrations. The response analysis consisted of the following steps:

- (1) Determine the rotor imbalance loads and the case impact loads for the equivalent fan disk fragments.
- (2) Perform the rotor/frame transient analysis to identify structural areas of concern under the loss of an equivalent disk fragment.
- (3) Identify potential solutions for the limiting structural components.

## 3.0 CONTAINMENT ANALYSIS

### 3.1 ENGINE CONTAINMENT

Damage to the aircraft may occur whenever a failure occurs in a rotating stage of a turbine engine. This damage which may be critical to the aircraft can be reduced by minimizing the number of failures, and by containing, within the engine nacelle any fragments resulting from a rotor stage failure.

#### 3.1.1 Description of Fragment

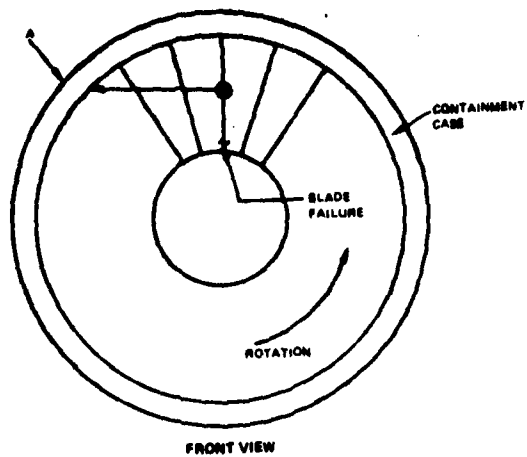
The engine containment analysis was based on a rotor failure which produces a disk fragment with energy equivalent to two adjacent blades with an included disk serration, and four adjacent blades with three included disk serrations. The severest occurrence for this type of rotor failure occurs with a disk serration failure which liberates the blades and serration(s) at the same instant of time. In reality, these types of disk failures could be equated to other types of disk failures on an equivalent energy basis.

The equivalent energy for these disk fragments was determined by summing the individual kinetic energy of each blade and disk serration for respectively the fan unit, the low pressure compressor unit, the high pressure compressor unit, the high pressure turbine unit and the low pressure turbine unit based on its own mass, velocity and center of gravity.

#### 3.1.2 Analytical Procedure for Fan Section

The analytical procedure used for the fan disk failure fragments is an extension of the fan blade containment analysis currently used at P&WA which recognizes that at the instant a fan blade fails, it moves in a tangential path due to the rotational speed of the rotor as shown in Figure 2 and impacts the containment case at point A. This tangential velocity component and the resulting fragment kinetic energy was used to calibrate the containment analysis. A calculation of the kinetic energy component due to the rotational velocity of the blade around its center of gravity shows the level to be approximately 10% of the tangential kinetic energy component. The rotational effects have been included as part of the empirical factor which relates the analytical results to actual blade failure experience. This experience has shown that the failed blade impacts the case several times, and during these impacts, the tip of the blade breaks away due to blade buckling as shown in Figure 3. Buckling ceases when the force required to buckle the remaining blade fragment exceeded the maximum impact force. The calculated tangential kinetic energy of the blade fragment was adjusted after each impact to account for the reduced mass and increased radius to the blade fragment center of gravity.

As part of the containment analytical procedure, the containment capability of the case (potential energy) was related to the energy required to punch out a "shear plug". The "shear plug" dimensions were defined by the blade perimeter and case thickness and represents the amount of case material that must be removed in order to let the blade pass through the case. The blade platform was ignored from the perimeter since its strength was negligible when compared with the case.



BLADE FRAGMENT KINETIC ENERGY - KINETIC ENERGY OF SINGLE BLADE FAILURE INCLUDING THE EFFECT OF BLADE BUCKLING



Figure 2 Fan Containment - Single Blade Failure

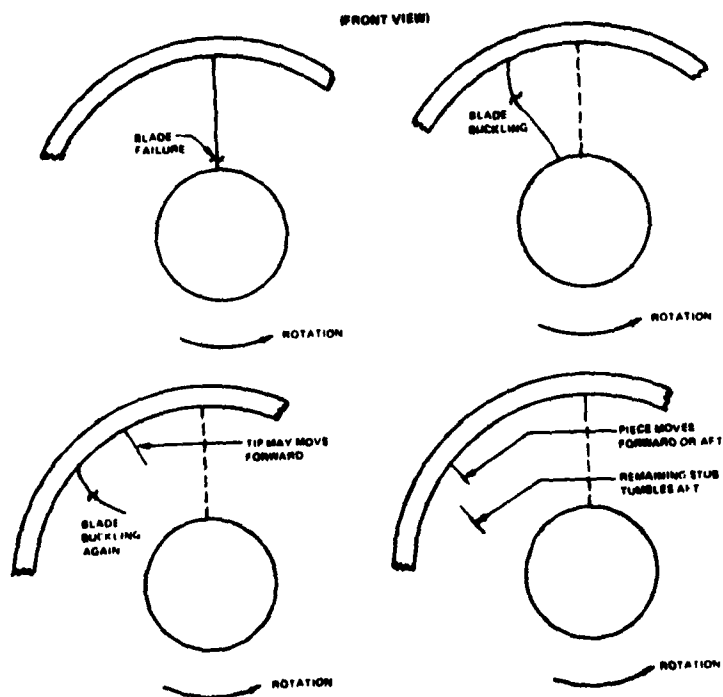


Figure 3 Fan Blade Buckling Upon Impact With the Containment Case

Multiple blade failures would be similar to a single blade failure since each blade behaves independently. For a failure where two adjacent blades fail, each blade fragment moves along its individual tangential path and impacts the containment case at different points (Points A and B shown in Figure 4). Blade buckling would be expected to be similar to that occurring with a single blade failure. The "shear plug" produced by each blade segment does not overlap and therefore the containment case designed for a single blade failure would be sufficient to contain a double fan blade failure. In addition, service experience on a variety of commercial engine models including the JT9D engine has demonstrated that blade fragments can be contained by the existing engine cases with no increase in engine weight.

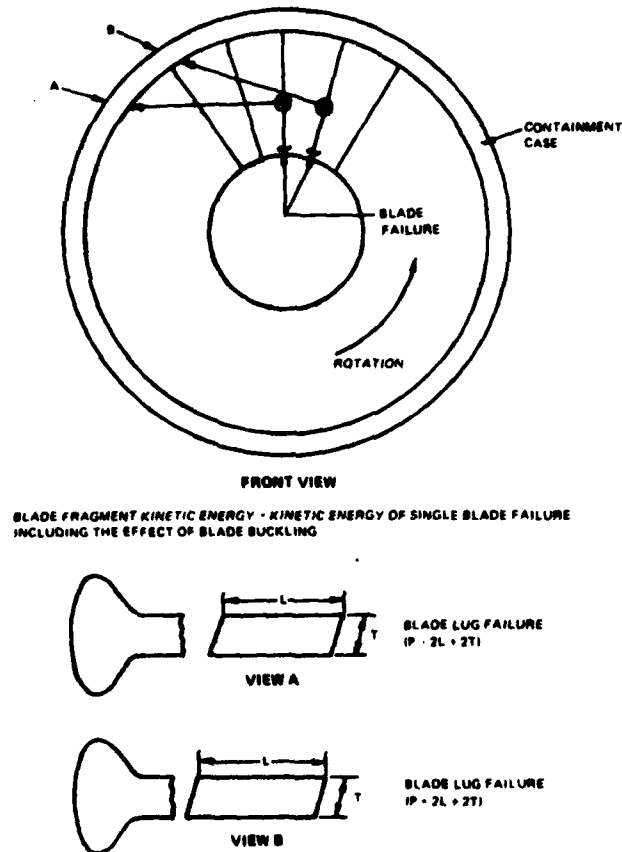


Figure 4 Fan Containment - Multiple Blade Failure

The disk fragments considered in this study were assumed to be the result of a disk failure with energy equivalent to two adjacent blades and an included disk serration, and four adjacent blades and their included disk serrations. The blades and disk serration(s) were considered as one fragment moving along a tangential path and impacting the containment case at point A shown in Figure 5. The tangential kinetic energy component of the blades and disk serration(s) were added as discussed in Section 3.1.1. Buckling of the blades was assumed to occur as in a single fan blade and the tangential kinetic energy of the fragment was adjusted for the reduced mass and increased radius to the center of gravity.

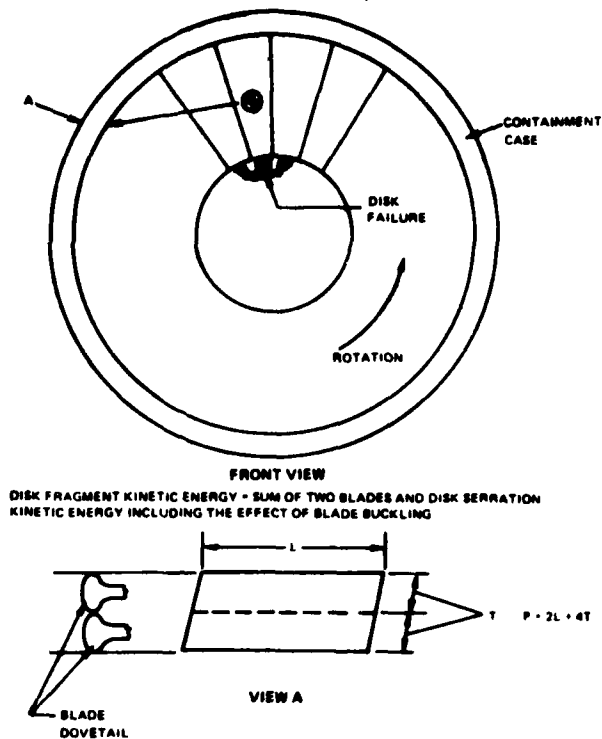


Figure 5 Fan Containment – Disk Fragment With Energy Equivalent to Two Adjacent Blades and an Included Disk Serration

The “shear plug” produced in the containment case by the equivalent disk fragments had a perimeter equal to the fragment. Thus, for the equivalent disk fragment of two blades and a disk serration, the perimeter was two times the dovetail length plus four times the dovetail thickness ( $2L+4T$ ) as shown in Figure 5 and not twice the perimeter of a single blade dovetail ( $4L + 4T$ ). This difference would also indicate that a noncontained failure with this fragment would produce a single puncture rather than two separate punctures. The disk serration was included in the kinetic energy but was assumed to have a negligible effect on the perimeter of the “shear plug” produced. The kinetic energy of the disk serration was approximately 1/16 the kinetic energy of the fan blade.

The analytical equation that was applied to the fan section is given below:

$$t^2 = \frac{F^2 B (KE)_T}{\tau_D P \phi}$$

where  $t$  = required minimum case thickness for containment

$F$  = empirically determined factor based on single blade failure experience.

**B** = buckling factor defined as the ratio of the fragment tangential kinetic energy after buckling has occurred to the fragment tangential kinetic energy prior to buckling

**(KE)<sub>T</sub>** = tangential kinetic energy of the fragment prior to buckling

**τ<sub>D</sub>** = dynamic shear strength of the case material

**P** = perimeter of the "shear plug"

**φ** = factor which related the mass of the "shear plug" produced in the containment case to the mass of the fragment =

$$1 + \frac{M \text{ shear plug}}{M \text{ fragment}}$$

**Aft Containment** – For a fan blade failure, aft containment in the region rearward from the leading edge of fan splitter to the forward section of the fan exit guide vanes, would be required to contain the remaining blade fragment or "stub" of a fan blade after buckling has occurred as shown in Figure 6. After several impacts of the fan blade with the containment case, and after buckling of the fan blade has occurred, the remaining blade fragment or "stub" tumbles rearward and impacts the fan cases in the aft location. Since the "stub" has reduced mass and energy, the required thickness is significantly reduced over the in-plane thickness. The required thickness was based on fan blade failure experience of comparable engine models.

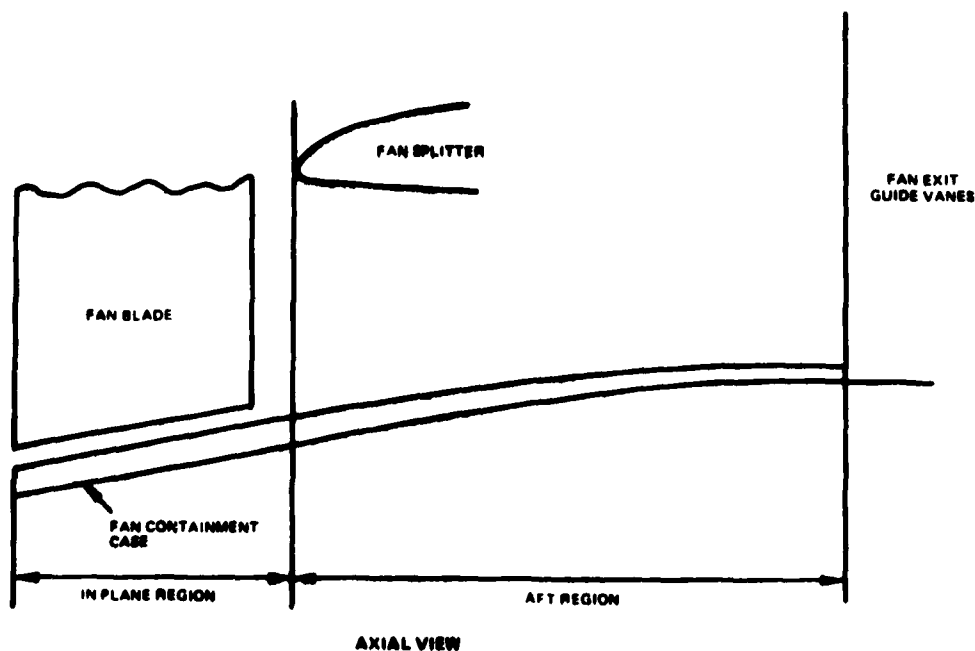
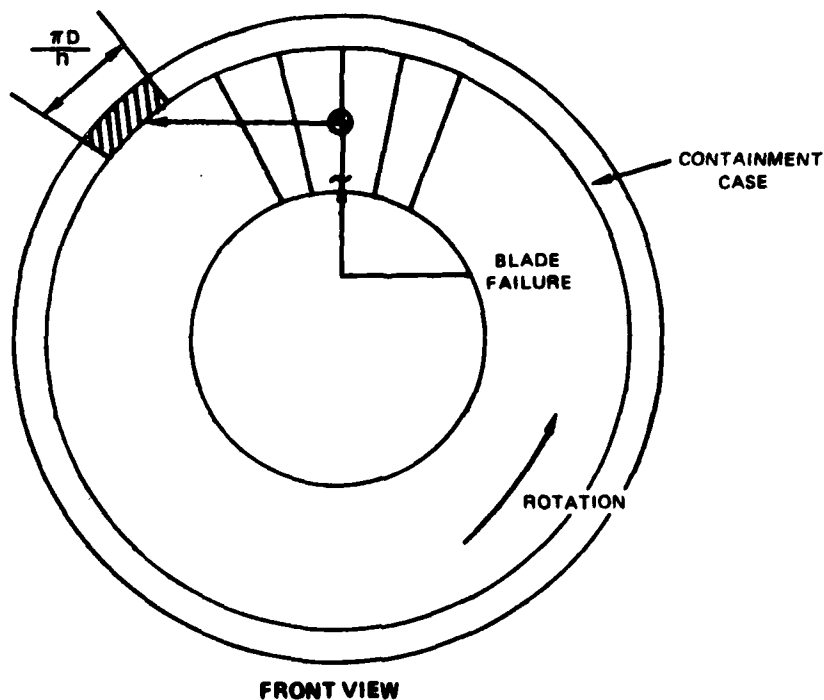


**Figure 6** Region of Aft Containment Required for Fan Blade Failures

The fragments directed rearward in this study were assumed to consist of the remaining fan blade "stubs", after fan blade buckling had occurred, and the disk serration. The kinetic energy of the equivalent fragment determined at the blade tip velocity of the fan rotor was the sum of each blade "stub" and disk serration kinetic energy. The required containment thickness was then assumed to be directly proportional to the square root of the remaining fragment kinetic energy.

### 3.1.3 Analytical Procedure for Compressor and Turbine Section

The analytical procedure used for the equivalent compressor and turbine disk failure fragments was an extension of the compressor and turbine blade failure fragment procedure currently in use. The blade fragment at the instant of failure moves in a tangential path and impacts the containment case as shown in Figure 7. Again the kinetic energy of the fragment considered in the analysis was associated with the tangential velocity component. Since the compressor and turbine blades are smaller than fan blades, the rotational kinetic energy component is a lower percentage of the tangential kinetic energy and is included in an empirical factor which relates the analytical results to the blade failure experience.

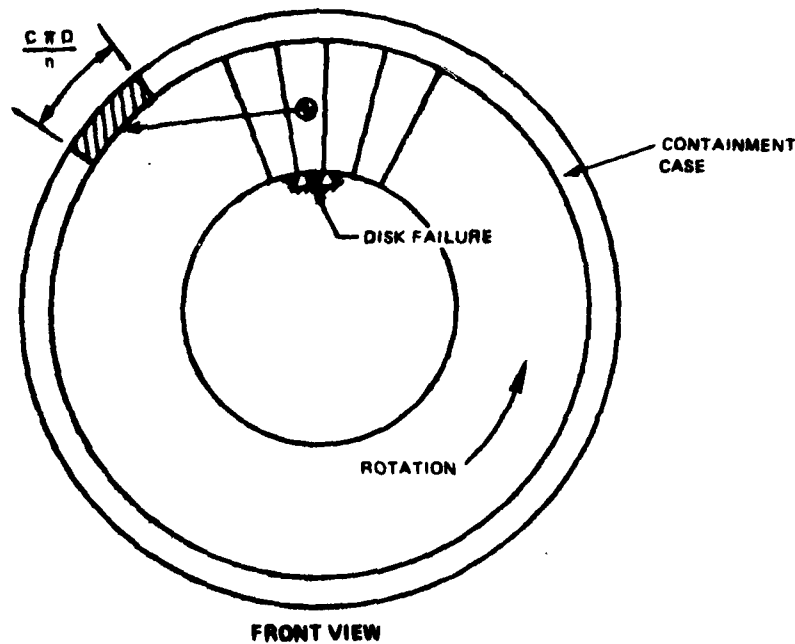


BLADE FRAGMENT KINETIC ENERGY - KINETIC ENERGY OF SINGLE BLADE FAILURE  
 $D$  - NOMINAL DIAMETER OF CONTAINMENT CASE  
 $n$  - NUMBER OF BLADES IN THE ROTOR STAGE

Figure 7 Compressor and Turbine Containment - Single Blade Failure

The containment capability of the case (potential energy) was assumed to be related to the hoop strain energy in the case. For a single blade, the effective circumferential length of the case material available for absorbing the fragment kinetic energy was one pitch length -  $\pi D/n$  where  $D$  is the nominal diameter of the containment case and  $n$  is the number of blades in the rotor stage.

For a disk fragment with the equivalent energy of two adjacent blades with an included disk serration, and four adjacent blades with three included disk serrations, the blades and disk serration(s) were considered as one fragment which moved along a tangential path and impacted the containment case as shown in Figure 8. The circumferential length of case material available for absorbing the disk fragment kinetic energy was increased compared to a single blade fragment by a nondimensional factor. This factor relates the effective circumferential length of case for a disk fragment to the one pitch circumferential length for a single blade fragment. In one extreme, increasing the circumferential length to two and four times the single blade pitch length for the two and four bladed disk fragments, respectively, would result in no additional weight required for containment. In the other extreme, assuming a single blade one pitch length would be too conservative and would result in unrealistic additional weight. The actual situation lies between these two extremes.



DISK FRAGMENT KINETIC ENERGY - SUM OF TWO BLADES AND DISK SERRATION KINETIC ENERGY

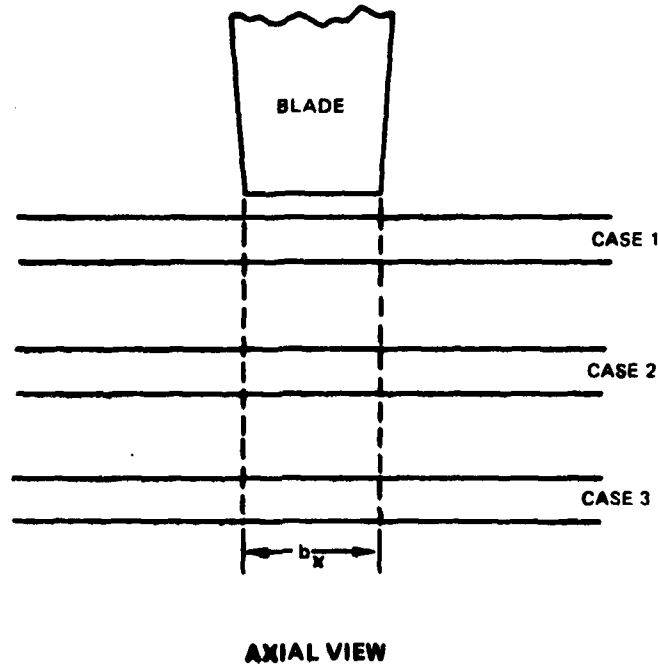
- D - NOMINAL DIAMETER OF CONTAINMENT CASE
- n - NUMBER OF BLADES IN THE ROTOR STAGE
- C - A NONDIMENSIONAL FACTOR WHICH RELATES THE EFFECTIVE CIRCUMFERENTIAL LENGTH OF CASE FOR A DISK FRAGMENT TO THE ONE PITCH CIRCUMFERENTIAL LENGTH FOR A SINGLE BLADE

Figure 8 Compressor and Turbine Containment - Disk Fragment With Energy Equivalent to Two Adjacent Blades and an Included Disk Serration



Based on limited service experience with similar type disk fragments, a factor of 1.3 and 2.0 was determined for the two and four bladed disk fragment, respectively. Since the kinematic action of the liberated fragment is complex, additional testing would be required to further substantiate these factors.

For containment the ratio of case potential energy to the fragment kinetic energy was based on an empirical factor obtained from experience with blade failures in the compressor and turbine sections. The total hoop potential energy was defined as the sum of each case hoop potential energy that lies within the radial plane of the blade as shown in Figure 9.



$$PE_{TOTAL} = \sum PE_{CASE} = \sum_{i=1}^m db_x \left( \frac{C \pi D_i}{n} \right) (M_i K_i)$$

Figure 9 Containment Capability of Compressor and Turbine Cases

The required containment case thickness was determined from the following equation:

$$CF = \frac{PE}{KE} = \frac{\sum_{i=1}^m db_x \left( \frac{C \pi D_i}{n} \right) (M_i K_i)}{(KE)_T}$$

$$CF = \frac{\Sigma(\text{Containment Volume}) (\text{Material Factor})}{\text{Fragment Tangential Kinetic Energy}}$$

where:

**CF** = required containment factor

**PE** = potential energy

**KE** = kinetic energy

**d** = factor relating to the effective axial length of case

**b<sub>x</sub>** = axial projection of the blade tip (see Figure 9)

**C** = a nondimensional factor which relates the effective circumferential length of case for a disk fragment to the one pitch circumferential length for a single blade

**t** = required minimum case thickness for containment

**D** = nominal diameter of the containment case

**n** = no. of blades in the rotor stage

**M<sub>f</sub>** = static material factor

**K** = dynamic factor

**(KE)<sub>T</sub>** = tangential kinetic energy of the fragment

### 3.1.4 Kinetic Energy Levels for the Disk and Blade Fragments

A disk fragment with energy equivalent to two blades with a disk serration is shown in Figure 10 for a typical turbine engine rotor. The weight of the fragment is the sum of the weight of the two whole blades and the disk serration assuming failure of the disk serration at the thinnest section. The tangential kinetic energy was calculated for the whole blade and disk serration separately by using the following equation:

$$(KE)_T = \frac{MV^2}{2}$$

where:

**(KE)<sub>T</sub>** = tangential kinetic energy

**M** = mass of the blade or disk serration

**V** = tangential velocity of the blade or disk serration at the center of gravity

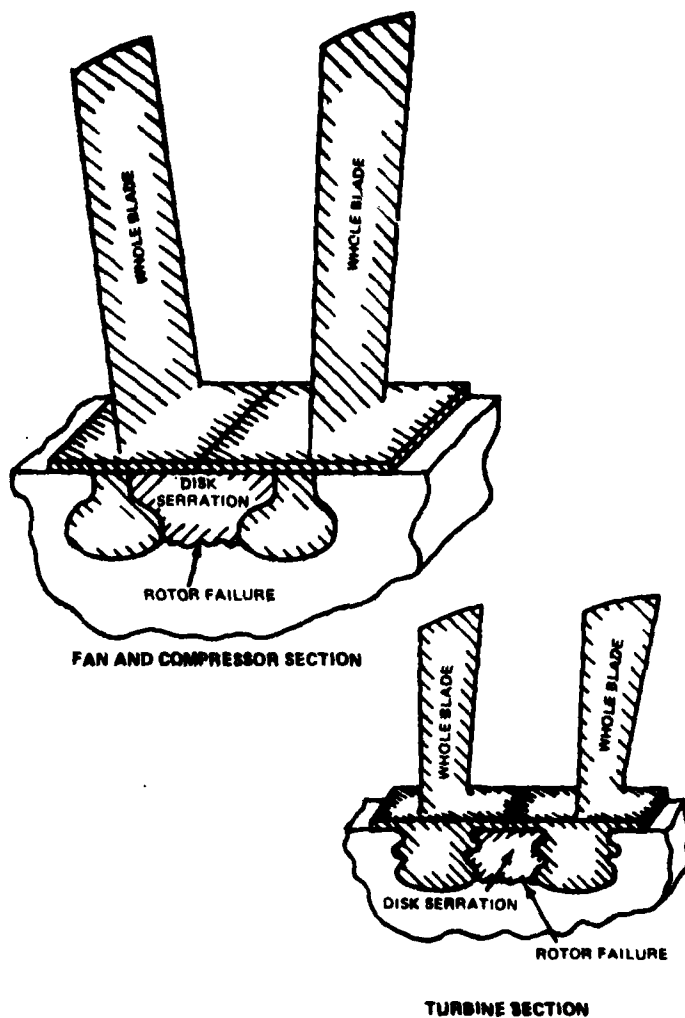


*Figure 10 A Two Blade and an Included Disk Serration Fragment From a Typical Turbine Engine Rotor*

The kinetic energy of the fragment was determined at the "red line" rotor speed by summing the kinetic energy for each blade and disk serration and is shown in Table 1. The largest weight and kinetic energy fragment was in the fan section as expected. Generally, the further rearward the rotor stages in the compressor section, the lower the weight and kinetic energy. The last two rotor stages in the compressor section showed an increase in weight and kinetic energy due to the transition from a titanium base alloy to a higher density nickel base blade alloy. The high pressure turbine section produced the second highest kinetic energy fragments due to the greater weight and radius to the center of gravity compared to the high pressure compressor stages. In the low pressure turbine section, the rearward stages showed increased kinetic energy due to the greater weight and radius to the center of gravity.

N<sub>1</sub> = 3700 rpm (Red Line)  
 N<sub>2</sub> = 8011 rpm (Red Line)

Rotor Group	Stage	Number of Blades	Single Rotor Blade		Disk Fragment 2 Blades & Included Disk Serrations		Disk Fragment 4 Blades & Included Disk Serrations		
			Weight (lbs.)	Energy (in-lbs.)	Weight (lbs.)	Energy (in-lbs.)	Weight (lbs.)	Energy (in-lbs.)	
Fan (N <sub>1</sub> )	1	46	9.490	1,590,000	20.70	3,250,000	43.12	6,600,000	
LPC (N <sub>1</sub> )	1.5	108	0.217	22,100	0.496	49,300	1.054	104,000	
	2	120	0.180	17,400	0.398	37,800	0.834	78,500	
	3	112	0.230	19,500	0.498	41,600	1.034	85,900	
	4	100	0.236	17,700	0.575	38,330	1.200	79,500	
HPC (N <sub>2</sub> )	5	60	0.253	43,300	0.603	101,000	1.304	215,000	
	6	84	0.130	22,200	0.290	48,700	0.608	101,700	
	7	102	0.070	12,200	0.155	26,700	0.324	55,500	
	8	100	0.052	8,730	0.113	18,800	0.236	39,000	
	9	110	0.042	6,990	0.091	15,000	0.189	31,100	
	10	108	0.037	6,070	0.081	13,200	0.169	27,500	
	11	104	0.037	5,990	0.082	13,100	0.171	27,400	
	12	94	0.037	5,930	0.084	13,400	0.178	28,200	
	13	100	0.034	5,400	0.083	12,900	0.180	28,000	
	14	102	0.065	10,300	0.144	22,700	0.302	47,500	
	15	90	0.075	11,900	0.170	26,800	0.360	56,500	
	HPT (N <sub>2</sub> )	1	100	0.300	121,000	1.21	292,000	2.55	616,000
		2	102	0.616	140,000	1.44	331,000	3.00	685,000
	LPT (N <sub>1</sub> )	3	122	0.302	20,600	0.637	42,800	1.31	87,200
		4	120	0.460	31,400	0.967	65,100	1.98	132,000
5		110	0.684	53,600	1.45	111,000	2.98	226,000	
6		102	0.988	85,300	2.07	177,000	4.22	359,000	

Table 1 Kinetic Energy Developed By a Disk Fragment Compared To a Single Blade Failure

### 3.1.5 Engine Case Materials and Maximum Operating Temperatures

The containment capability of the engine cases is a function of the material dynamic shear strength used in the fan section and the material factor used in the compressor and turbine section. The dynamic shear strength and material factors were chosen by considering minimum material strength at the hottest operating temperature. Using maximum engine operating temperatures and the resultant lowest material factors, containment of the fragments at other engine operating conditions with lower temperatures would be ensured. The engine case materials and maximum operating temperatures are shown in Table 2. The inner structure refers to the engine case closest to the rotor blade tip, while the outer structure refers to the remaining engine cases.

<u>Section</u>	<u>Case Materials</u>	
	Fan	410 Type Stainless Steel (In-Plane)
Low Pressure Compressor	6061 Type Aluminum Alloy	
High Pressure Compressor	410 Type Stainless Steel (Front Stages)	
	Titanium Base Alloy (Front Stages)	
	430 Type Stainless Steel (Middle Stages)	
	Titanium Base Alloy (Middle Stages)	
High Pressure Turbine	Nickel Base Alloy (Rear Stages)	
	Cobalt Base Alloy	
	Nickel Base Alloy	
Low Pressure Turbine	Nickel Base Alloy	
	Greek Ascoloy Stainless Steel (Rear Stage)	
	<u>Case Temperatures</u>	
	<u>Inner Structure</u>	<u>Outer Structure</u>
Fan	200°F	None
Low Pressure Compressor	250°F - 350°F	250°F
High Pressure Compressor	400°F - 1050°F	250°F - 850°F
High Pressure Turbine	1600°F	900°F - 1050°F
Low Pressure Turbine	950°F - 1200°F	None

*Table 2 Engine Case Materials and Maximum Operating Temperatures*

### 3.1.6 Additional Weight for Containment of Disk Fragment with Energy Equivalent to Two Adjacent Blades and an Included Disk Serration

Aircraft turbine engines are presently designed to provide containment of blade failures. The weight required to contain blade failures and the weight already provided within the plane of the rotor stage were determined and are shown in Table 3. For all engine rotor sections, the weight provided exceeds the weight required for containment. The reason for this is that the case sizes are limited by other design criteria. Table 4 shows the additional weight of engine cases required to contain a rotor fragment with energy equivalent to two adjacent blades and an included disk serration. The analytical procedures in Section 3.1.2 and 3.1.3 were used to determine the capability of the existing engine cases and the additional weight required for increased containment.

Location	Containment Weight Required	Containment Weight Provided <sup>a</sup>
Fan (including aft containment)	240 lbs.	300 lbs.*
LPC	25	50
NPC	20	65
HPT	40	50
LPT	40	45
TOTAL	365	510

\*Cases sized to satisfy other design criteria.

**Table 3 Engine Weight Necessary To Satisfy Present Blade Containment Requirements**

Fan Rotor	Single Blade Disk Fragment	Kinetic Energy (in-lbs)			Additional Weight (lbs)	
		$1.59 \times 10^6$	$3.25 \times 10^6$	In-Plane Aft	65 60	125
LPC Rotor	1.5C	18,900*	12,300	0	0	0
	2C	12,000*	9,500	0	0	0
	3C	4,900	10,400	5,500	10	10
	4C	5,800	9,500	3,700	5	15
*Includes additional material required for fan containment						
NPC Rotor	5C	25,600	25,200	0	5-7C	0
	10C	3,400	3,300	0	8-13C	0
	14C	7,500	5,700	0	14,15C	0
					Total	0
HPT Rotor	1T	14,200	15,000	20,800		25
	2T	22,900	19,700	16,800		20
					Total	45
LPT Rotor	3T	3,100	5,100	2,000		5
	4T	3,400	7,800	4,400		10
	5T	4,100	13,300	9,200		15
	6T	14,400	21,200	6,000		10
					Total	40
Total Additional Weight for Containment						≈ 220
Containment Weight Provided						510
Total Engine Containment Weight						≈ 730

**Table 4 Additional Weight For Containment of a Disk Fragment With Energy Equivalent To Two Adjacent Blades and an Included Disk Serration**

In the fan section, the kinetic energy of the rotor fragment is more than twice the kinetic energy of a single blade. The additional weight is essentially evenly split between the in-plane and aft sections.

In the compressor and turbine sections, a comparison is made between the available existing case potential energy and the required case potential energy. Additional weight is required in those stages where the available case potential energy is insufficient to contain the equivalent disk fragment. Only selected stages were calculated in the HPC section since the additional weight required was relatively smaller than the other engine sections.

The fan section requires the largest additional weight. This appears reasonable since the fan rotor fragment possesses the highest kinetic energy. The second largest additional weight occurs in the HPT section where the fragment possesses the second highest kinetic energy. Similarly, the least additional weight occurs in the HPC section where the fragment possesses the lowest kinetic energy.

The total engine weight required for containment of the two bladed disk fragment was approximately 730 pounds compared to 365 pounds for the present requirements. The total additional weight, beyond what is provided presently in the engine was approximately 220 pounds.

### **3.1.7 Additional Weight for Containment of Disk Fragment with Energy Equivalent to Four Adjacent Blades and Three Included Disk Serrations**

Table 5 shows the additional weight of engine cases required to contain a rotor fragment with energy equivalent to four adjacent blades and three included disk serrations. The available case potential energy and the required case potential energy increased for the larger fragment. The additional weight necessary to contain the four bladed disk fragment was much greater than the two bladed disk fragment.

Like the two bladed disk fragment, the additional weight for containment was largest in the fan section, second largest in the HPT section, and the least in the HPC section. The total engine weight required for containment of the four bladed disk fragment was approximately 920 pounds compared to 365 pounds for the present requirements. The total additional weight, beyond what was provided, was approximately 410 pounds.

### **3.1.8 Additional Weight for Low Pressure Compressor Section with Alternate Engine Case Materials**

Maintaining the present case configuration, the additional required containment capability may be gained for a lower weight by adding an additional case made of a more efficient containment material directly behind the present cases. Table 6 shows the additional engine case weight required to contain a low pressure compressor equivalent disk fragment with alternate type case materials. The existing case material is a 6061 type aluminum alloy with an additional weight of 15 pounds and 25 pounds required for containment of the two bladed and four bladed disk fragment respectively. Both a 410 type stainless steel and a titanium base alloy additional case offers a significant weight savings potential. A decrease in weight for containment of approximately 10 pounds and 15 pounds was determined for the two bladed and four bladed disk fragment, respectively. Unlike for the fan section, where titanium would be lighter than stainless steel, the additional weight for these two case materials is the same since the difference in weight density is offset by the differences in material capability (material factor in Section 3.1.3).

Fan Motor	Single Blade Disk Fragment	Kinetic Energy (in-lbs)		In-Plane Aft	Additional Weight (lbs)		
		$1.50 \times 10^6$	$0.40 \times 10^6$		100	100	
					Total	200	
LPC Motor	Stage	Available Case P.B. (in-lbs)	Required Case P.B. (in-lbs)	$\Delta P.E.$ (in-lbs)	Additional Weight (lbs)		
		1.3C	30,200*	26,000	0	0	0
		2C	34,800*	19,600	0	0	0
		3C	7,500	21,300	14,000	15	15
		4C	9,000	19,900	10,900	10	10
	Total					25	
*Includes additional material required for fan containment							
NPC Motor	Stage	5C	39,400	53,700	14,300	5-7C	10
		10C	5,300	6,800	1,500	8-13C	5
		14C	11,600	11,900	300	14,19C	1
	Total					16	
NPT Motor	Stage	17	21,800	73,900	52,100		40
		2T	33,200	82,200	47,000		35
		Total					75
LPC Motor	Stage	3T	4,800	10,500	5,700		5
		4T	5,300	15,800	10,500		10
		5T	6,300	27,100	20,800		20
		8T	22,200	43,100	20,900		25
		Total					60
Total Additional Weight for Containment						≈ 410	
Containment Weight Provided						510	
Total Engine Containment Weight						≈ 920	

**Table 5 Additional Weight for Containment of a Disk Fragment With Energy Equivalent To Four Adjacent Blades and Three Included Disk Serrations**

**Disk Fragment (Energy Equivalent to Two Adjacent Blades and Disk Serrations)**

Stage	Existing 6061 Type Aluminum Alloy	410 Type Stainless Steel	Titanium Base Alloy
1.3C	0	0	0
2C	0	0	0
3C	10	3	3
4C	5	2	2
Total	15	5	5

**Disk Fragment (Energy Equivalent to Four Adjacent Blades and Three Disk Serrations)**

Stage	Existing 6061 Type Aluminum Alloy	410 Type Stainless Steel	Titanium Base Alloy
1.3C	0	0	0
2C	0	0	0
3C	15	5	5
4C	10	4	4
Total	25	9	9

**Table 6 Additional Weight To Contain a Low Pressure Compressor Disk Fragment With Alternate Engine Case Type Materials**



### **3.1.9 Design Considerations and Limitations**

The kinetic energy of disk fragments require additional weight for containment beyond that provided by the existing engine cases. Further additional weight which lies outside the radial plane of the rotor stage is necessary because:

- (1) Engine case thermal stresses and resulting safe operating lives are affected because of the thermal gradients produced between the very thin to thick cross-sections in the case.
- (2) Case bolting and other hardware have to be modified in order to carry the increase in impact load.

The increase in weight is approximately 25 percent for the two blade fragment and approximately 35 percent for the four blade fragment. The total increased case thicknesses in turn will have an effect on other engine design considerations and limitations as discussed below:

- (1) Engine seal clearances would change because of changes in the thermal response of the engine cases. The thick cases would have a slower growth response and cause the blade tips to rub, thus opening the blade tip clearance. The engine performance and surge margins would be significantly affected.
- (2) Case natural frequencies would change due to the added weight plus all case responses to engine excitations (example, blade passing frequency) would have to be rechecked.
- (3) Engine assembly would become more complex due to changes required in plumbing, bolting and handling the heavier cases.
- (4) Ultimate increase in cost to the consumer would result because of the increase in weight and fundamental performance disadvantage of thick engine cases.

## **3.2 FORWARD CONTAINMENT**

The cases that currently provide forward containment are not a part of P&WA engine hardware. However, for this study forward containment was assumed to be provided by a case made of engine case materials.

### **3.2.1 Description of Fragment**

From observations of cowl damage, there appears to be two types of blade tip fragments that may travel forward of the fan rotor radial plane. One type of fragment occurs as the tip section of the blade buckles and breaks away during impact of a failed fan blade with the in-plane containment case as shown in Figure 3. The other type occurs when leading edge pieces at or near the blade tip break off as shown in Figure 11 by bird strikes or other F.O.D. These fragments would be often reingested into the engine, striking the remaining fan blades and deflected forward again.

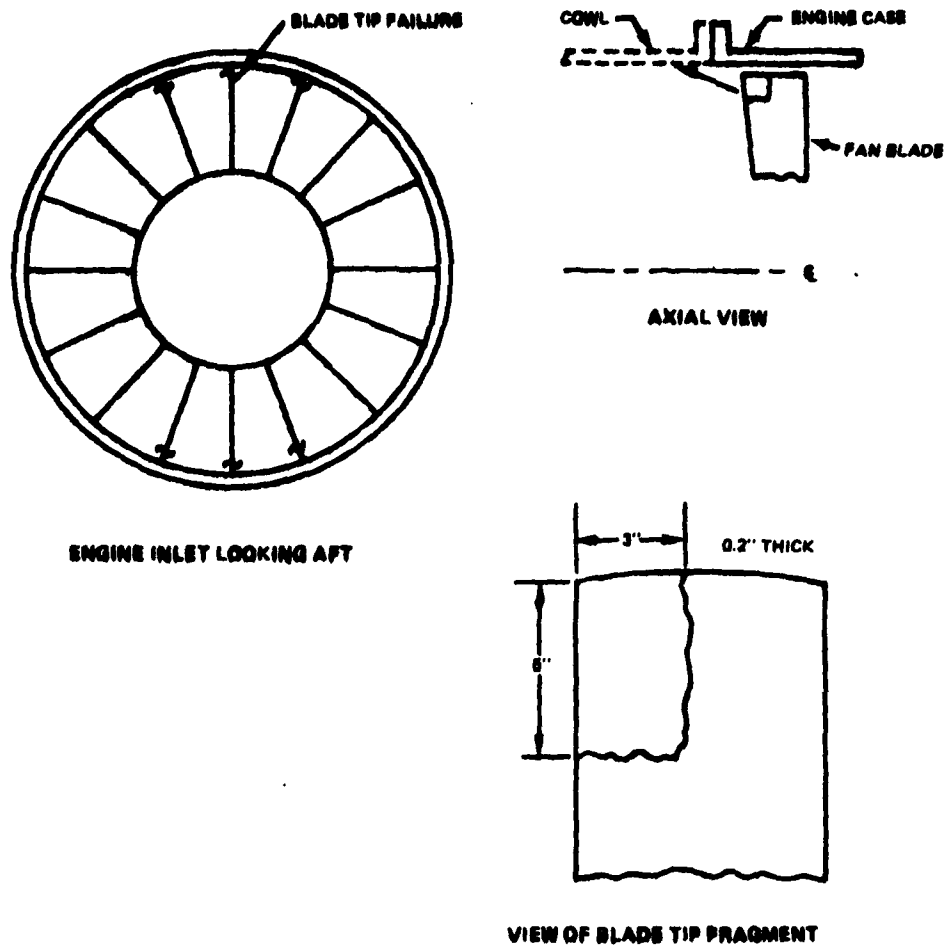


Figure 11 Description of Fan Blade Tip Fragment for Forward Containment

Observation of cowl damage also indicated two types of damage. First, the pieces that initially break from the fan blade tip produce a spiral slashing/cutting type puncture as the blade fragment travels forward parallel to the case surface. Second, the pieces that would be re-ingested into the engine and deflected forward again by the remaining fan blades produce a "punch out" type puncture of the case. Here the fragment trajectory would be more normal to the surface, producing a more conventional blade impact. Both these types of fragments shown schematically in Figure 12 were evaluated in this study.

The fan blade tip fragment evaluated in this study is shown in Figure 11. The six titanium pieces, three from three adjacent fan blades and the remaining three from three adjacent fan blades 180° away, were each 3" x 5" x 0.2" in size. Based on service experience, each fragment was assumed to act independently of each other and therefore impacted the forward containment case at random locations. On this basis, the weight of casing required to contain or deflect a single blade tip fragment up to 30° forward of the plane of rotation was determined.

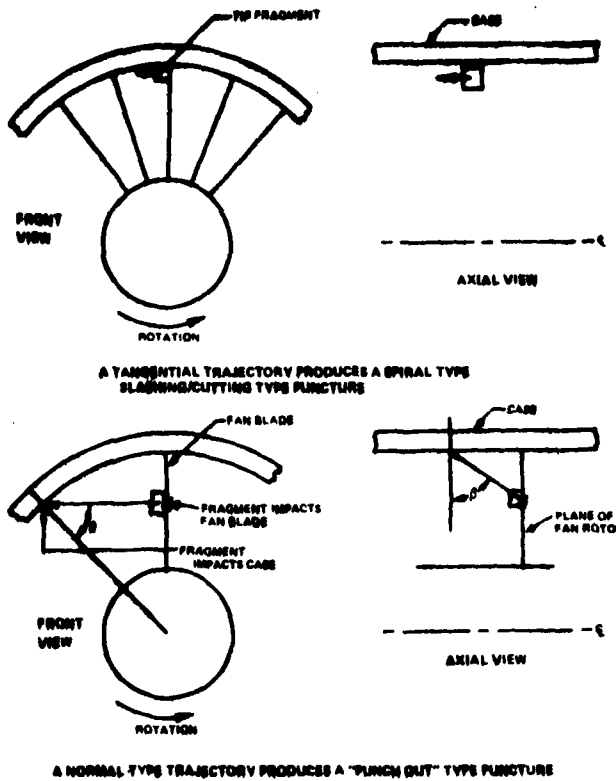


Figure 12 Fan Blade Tip Fragment Trajectories and Types of Case Damage

### 3.2.2 Analytical Procedure

The containment capability of the case (potential energy) was assumed to be related to the energy required to punch out a "shear plug" similar to the analytical procedure used for in-plane containment in the fan section. The equation used in this study is given below:

$$t^2 = \frac{(KE) \cos^2 \theta \cos^2 \beta}{\tau_D P \phi}$$

where:  $t$  = required minimum case thickness for containment

KE = kinetic energy of the forward moving fragment

$\theta$  = angle between the fragment tangential trajectory component and a normal to the case at the point of impact (see Figure 12)

$\beta$  = angle between the fragment axial trajectory component and a normal to the case at the point of impact (see Figure 12)

$\tau_D$  = dynamic shear strength of the case material

P = perimeter of the "shear plug"

$\phi$  = factor which relates the mass of the "shear plug" produced in the containment case to the mass of the fragment =

$$1 + \frac{M \text{ shear plug}}{M \text{ fragment}}$$

The above equation was compared with actual test data received from an aircraft manufacturer who under a similar FAA contract performed actual tests on simulated blade tip fragments. The tests conducted involved trajectory angles normal, 60° and initially parallel to a curved forward containment test panel. For the simulated blade fragment initially parallel to the curved containment panel, an angle of 80° was found to predict the test data. The results of the testing and the analytical predictions were in reasonable agreement.

### 3.2.3 Kinetic Energy of Forward Moving Fan Blade Fragments

The kinetic energy of a fan blade tip spiral slashing/cutting type fragment was determined based on the tangential velocity of the fan blade tip at the "red line" rotor speed. The axial velocity of the blade tip at the instant of failure would be zero and does not contribute to the kinetic energy. The calculated tangential velocity and kinetic energy was 18,500 in/sec. and 213,000 in-lbs., respectively. The weight of the 3 in. x 5 in. x 0.2 in. titanium blade tip fragment was determined to be 0.48 pounds based on a weight density of 0.160 pounds per cubic inch.

The kinetic energy of a single fan blade tip reingested "punch out" type fragment was determined based on the vector sum of the tangential velocity component and the forward axial velocity component which the fragment attains upon impact with the remaining fan blades. The tangential velocity at the "red line" rotor speed is shown in Figure 13 as a function of the radial reingestion location with the remaining fan blades.

For the reingested "punch out" type fragment that impacts the containment case at the fan blade rotor plane (angle  $\beta = 0$ ) the axial velocity is zero. The kinetic energy for this fragment reaches a maximum at the foil tip radius of 213,000 in-lbs. as shown in Figure 14. Note that this is the same kinetic energy level as the spiral slashing/cutting type fragment.

The reingestion of a fan blade tip fragment and the resulting forward trajectory is complex and random in nature. Simplifying assumptions were made to determine the kinetic energy and the impact angles relative to the containment case. A straight line trajectory was assumed from the radial reingestion location on the remaining fan blades to the impact location on the containment case. The forward axial velocity component and the tangential velocity component were initially assumed unaffected by aerodynamic drag. It was evident that this approach was too conservative when the calculated case thickness required for containment at the 30 degree forward axial location was much greater than required as indicated by successful service experience. Observations of cowl damage have shown that the existing cowl was sufficient to contain the forward moving fragments.

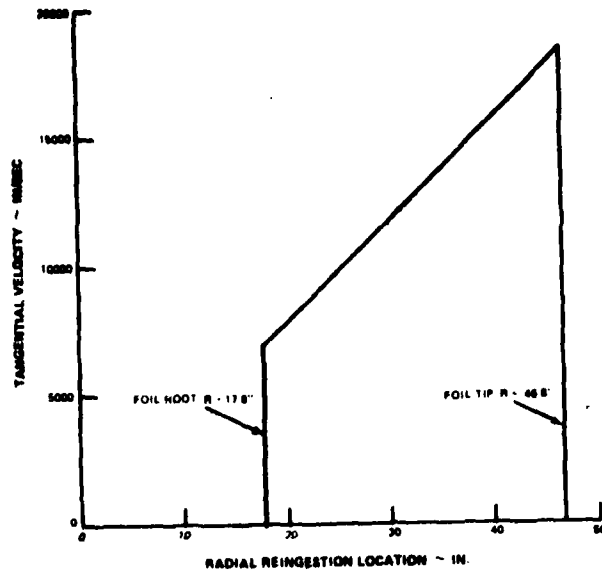


Figure 13 Fan Forward Containment – Tangential Velocity vs. Radial Reingestion Location for the “Punch Out” Type Fragment

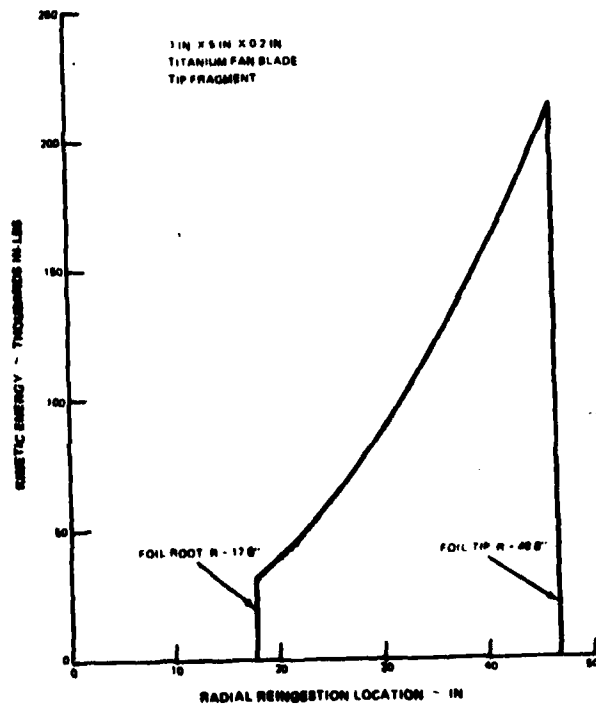


Figure 14 Fan Forward Containment – Kinetic Energy vs. Radial Reingestion Location for the “Punch Out” Type Fragment in the Fan Rotor Plane

To account for this good containment experience at the 30 degree forward location, the trajectory velocity was reduced at axial locations further forward of the fan until at the 30 degree location a trajectory impact velocity of approximately 15 percent of the value initially calculated was used. The 15 percent was determined by calculating the trajectory velocity that can be contained by the existing inlet cowl structure.

Figure 15 shows the trajectory velocity at the 30 degree forward location as a function of the radial reingestion location on the remaining fan blades. The maximum trajectory velocity was limited to 4700 inches per second since any greater velocity would require the blade tip fragment to be moving faster than the rotor velocity and air inlet airflow velocity.

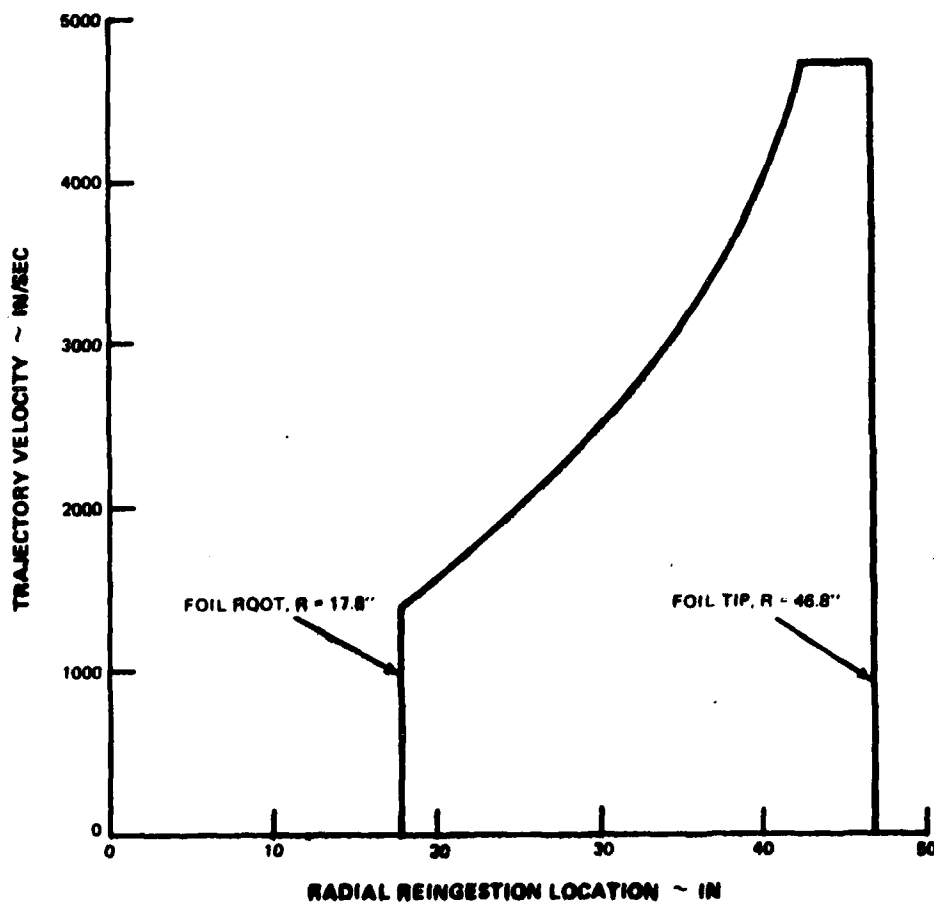


Figure 15 Fan Forward Containment - Trajectory Velocity vs. Radial Reingestion Location for Impact at 30 Degrees Forward of the Fan Rotor Plane

The kinetic energy of the reingested "punch out" type fragment as shown in Figure 16 increases with increasing radial reingestion location and would be limited to a maximum of 13,700 inch-pounds near the blade tip radius due to the trajectory velocity limitations.

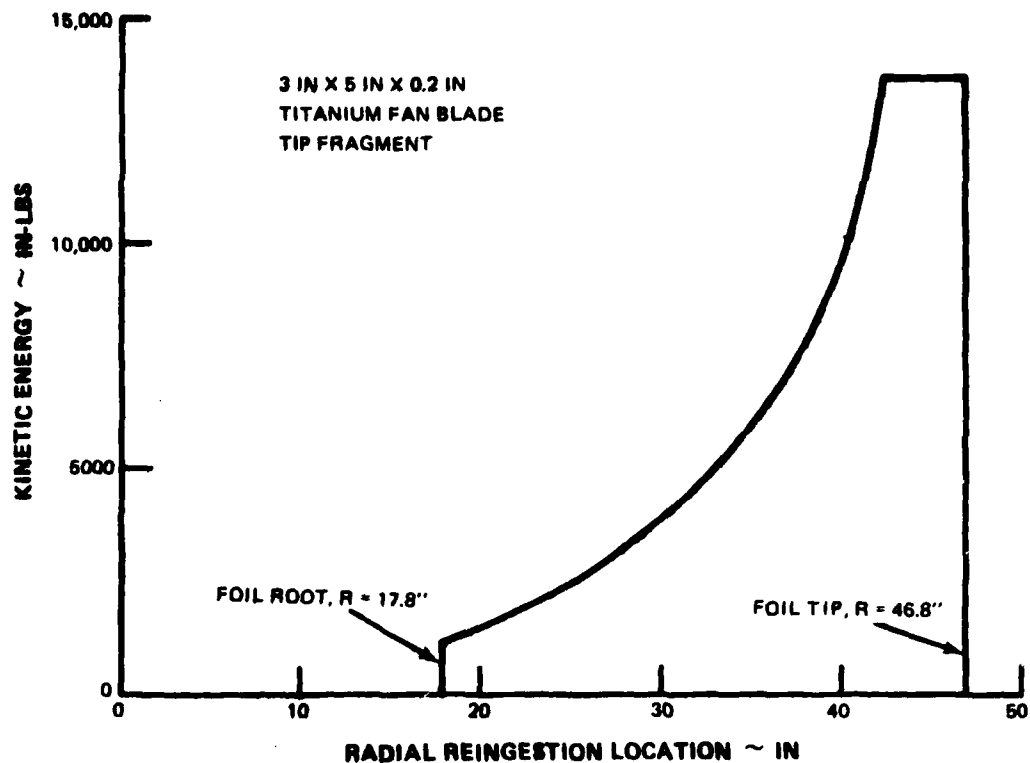


Figure 16 Fan Forward Containment – Kinetic Energy vs. Radial Reingestion Location for Impact at 30 Degrees Forward of the Fan Rotor Plane

### 3.2.4 Additional Weight for Containment

The case thickness required to contain the spiral slashing/cutting type fragment was determined using an angle  $\theta$  of 80 degrees based on the forward containment test results. The angle  $\beta$  does not enter into the calculation since the axial velocity is parallel to the containment case. The calculated case thickness necessary for containment was 0.049 in. and 0.060 in. for 410 type stainless steel and titanium alloy case materials, respectively. As the fragment spirals forward over the inlet containment case, the velocity will decrease rapidly due to the aerodynamic drag and friction from rubbing against the case.

The case thickness required to contain the reingested "punch out" type fragment was determined using the angle  $\theta$  shown in Figure 17. The angle  $\theta$  was derived from the radial reingestion location on the remaining fan blade and the location of impact with the inlet containment case (see Figure 12). As the radial reingestion location approaches the foil tip radius, angle  $\theta$  approaches 90 degrees indicating a tangential type of impact. Again, based on forward containment test data, angle  $\theta$  was limited to 80 degrees maximum.

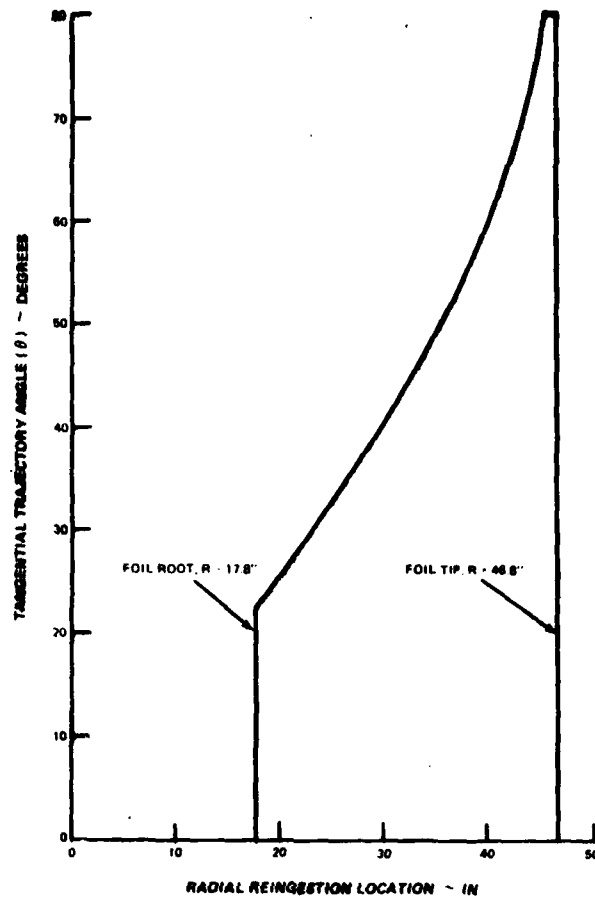


Figure 17 Fan Forward Containment -- Tangential Trajectory Angle vs. Radial Reingestion Location

The case thickness required to contain the reingested "punch out" type fragment in-plane with the fan blades is shown in Figure 18. The angle  $\beta$  is zero since the forward axial velocity component is zero by definition. The maximum thickness occurred at a radial reingestion location of approximately 33 inches which was about mid-span of the remaining fan blades. Near the foil tip, the calculated thickness was limited by the 80 degree maximum angle.

At the 30° forward axial location, the angle  $\beta$  was derived from the radial reingestion location with the remaining fan blades and the 30° forward axial location. Figure 19 shows the angle  $\beta$  as a function of radial reingestion location. Similarly, the angle  $\beta$  was limited to an 80 degree maximum. The case thickness required to contain the ingested "punch out" type fragment is shown in Figure 20. The maximum thickness occurs at a radial reingestion location of approximately 25 inches as measured from the engine centerline which is about one-quarter the span from the blade foil root to the blade foil tip. The case thickness required for containment was 0.017 and 0.021 for 410 type stainless steel and titanium alloy case material, respectively. In practice, if a conventional steel or titanium engine case were to provide the containment, the case thicknesses would be substantially greater than 0.017 and 0.021 due to manufacturing limitations.



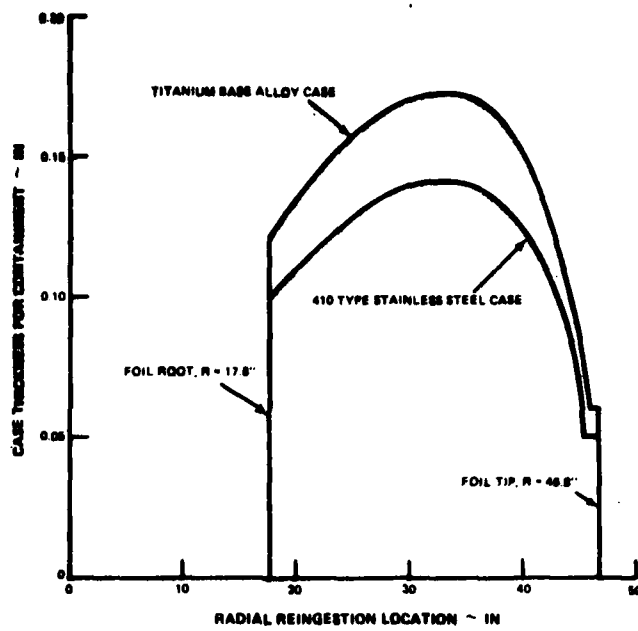


Figure 18 Fan Forward Containment – Case Thickness for Containment vs. Radial Reingestion Location for the “Punch Out” Type Fragment at the Fan Rotor Plane

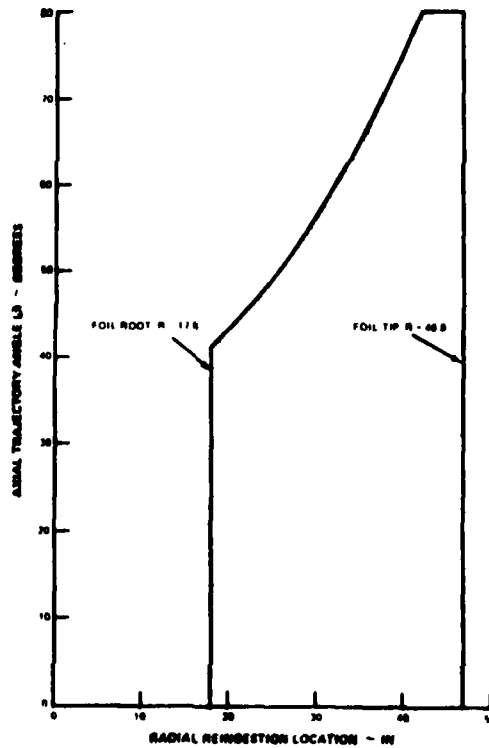
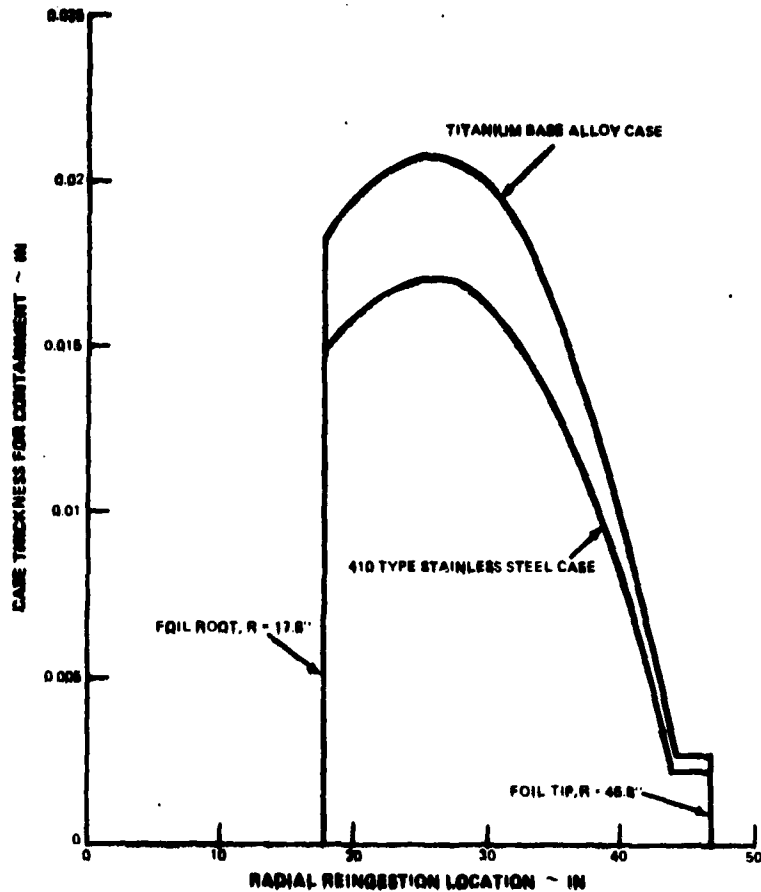


Figure 19 Fan Forward Containment – Axial Trajectory Angle vs. Radial Reingestion Location for Impact at 30 Degrees Forward of the Fan Rotor Plane



*Figure 20 Fan Forward Containment – Case Thickness for Containment vs. Radial Reingestion Location for Impact at 30 Degrees Forward of the Fan Rotor Plane*

The calculated case thickness required to contain the fan blade tip fragment as a function of axial distance is shown in Figure 21. The reingested "punch out" type fragment requires greater case thickness than the spiral slashing/cutting type fragment. The thickness required for the spiral slashing/cutting type fragment decreases with increasing forward location since the fragment velocity decreases due to frictional and aerodynamic forces. Thus, the thickness required for the reingested "punch out" type fragment sets the thickness for containment.

A case weight of 135 pounds for 410 type stainless steel and 105 pounds for titanium alloy case material was determined based on a linear case thickness distribution from the engine inlet flange to the 30 degree forward location. The axial distance between the fan blade rotor plane and the engine inlet flange was not included since the existing case thickness is sufficient to contain the fan blade tip fragment.

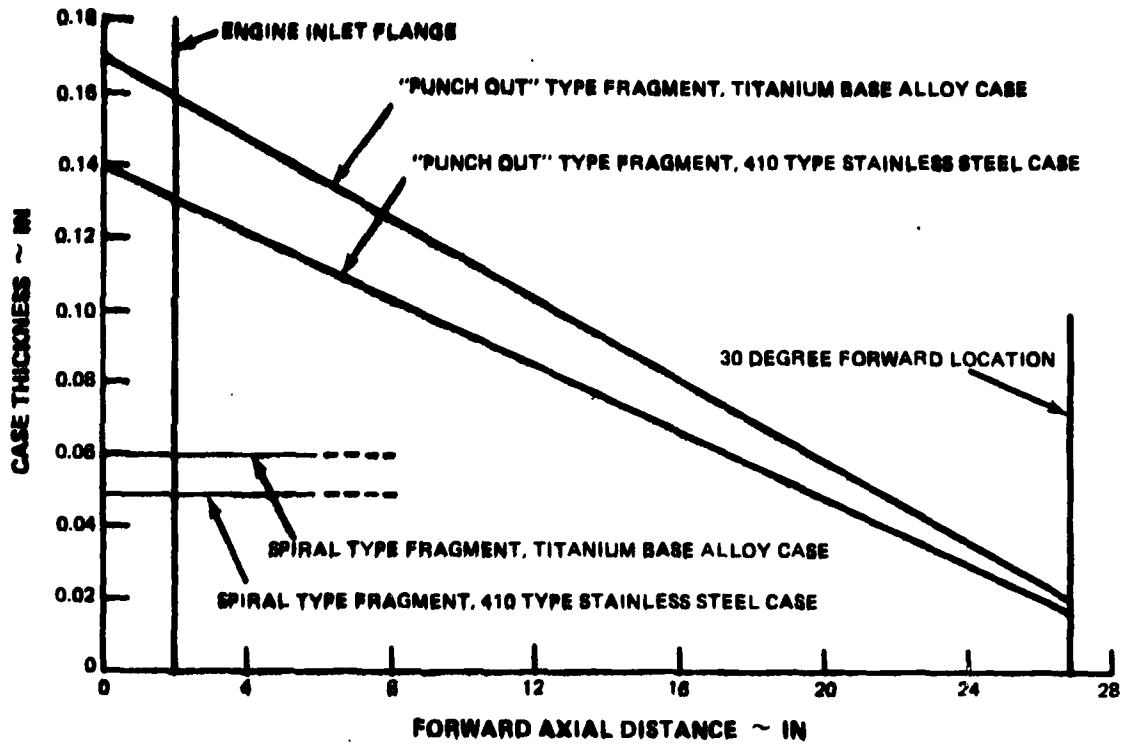


Figure 21 Fan Forward Containment - Case Thickness for Containment vs. Forward Axial Distance

## 4.0 TRANSIENT RESPONSE ANALYSIS

### 4.1 ANALYTICAL PROCEDURE

In addition to the in-plane containment requirements for any liberated fragments, the entire engine structure must be able to sustain the resulting rotating imbalance loads caused by the missing fragments in combination with the impact load produced by the liberated fragments striking the containment case.

#### 4.1.1 Description of Analysis

An analysis to determine the transient response of damped multi-rotor systems has been developed at Pratt & Whitney Aircraft and reported in Reference 1. In the analysis, rotor systems are idealized as rotating concentrated masses connected by massless beams, discrete springs and dampers. The springs may have bilinear springrates to simulate the effect of parts coming into contact after displacement through an initial clearance thereby creating alternate load paths (e.g. blade tips contacting cases).

The engine, shown schematically in Figure 22, was modeled as a 372 degree of freedom system (186 masses with two degrees of freedom each) with the connecting springrates, which represent bearings, struts, mounts, etc., determined from analysis and test data. Also included in the model were viscous dampers which provided a damping force that was proportional to the relative velocity between the damper end points. Test data for engine response to a known imbalance was used to determine the damping necessary in the analysis to duplicate the engine experience.

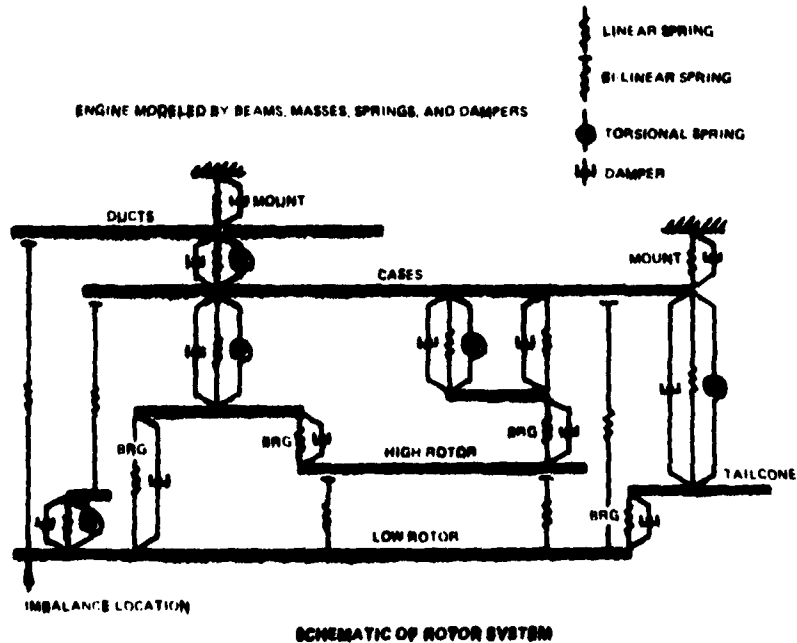


Figure 22 Schematic of Rotor System for Transient Response Analysis

#### 4.1.2 Assumptions in the Analysis

The springrates used to simulate rotor/rotor and rotor/case interferences were selected to match rub locations and rub depths observed from field experience for a single fan blade failure. It was assumed that the springrates were not variable and could also be used for the fan rotor failure analysis.

The analysis was performed for the existing engine configuration to identify structural areas of concern. The engine natural frequencies were not re-calculated with the "beefed-up" components due to the lengthy procedure necessary to iterate on the loads as the structure stiffness changed. Also, the containment case thicknesses for the study loadings were not defined at that point in time. The analysis identified those structural members which were marginal or inadequate for loads resulting from a fan rotor failure.

Minimum static material strengths were used to calculate the capability of all engine components. For some of the engine materials, an increase in material strength could be realized due to the rapid application of the loads, but a conservative approach of not accounting for any increases in material strength due to increased strain rates was taken because of the lack of sufficient dynamic material strength data.

#### 4.1.3 Case Impact Loads

To simulate the liberated fragments striking the containment case, an impulse force was applied to the case in the analysis. The magnitude of the force was determined from the momentum of the fragment and the time duration. The angular position of the force relative to the imbalance was determined from high speed motion pictures of a single fan blade failure. Figure 23 illustrates the force-time curve as well as the angular relationship between the imbalance and the impact force that was used in the analysis. The shape of the force vs. time impact was unimportant in the analysis since the time over which the force acted was very small compared to the period of the system natural frequencies.

#### 4.1.4 Alternate Load Paths

During the transient response of an engine, rotor/rotor and rotor/case interferences may occur. These interferences both limit the rotor excursions as well as provide alternate load paths to ground and must be included in a response analysis. As an example, the bearing load may be significantly reduced (Figure 24) if the shaft deflection is limited by interference rubs and a portion of the load that would normally be taken through the bearing to ground, is taken through the cases to ground. Conversely, the case loads may be significantly increased due to the additional load imposed at the interference location. Failure to account for these interferences will result in erroneous loads and deflections leading to either overdesign or underdesign of engine components.

Springs with piecewise linear springrates (bilinear) as shown in Figure 25 were included in the analysis at nine possible rub locations — fan, two low compressor stages, two low turbine stages, two high turbine stages, and two intershaft locations. The clearance at each possible rub location was set to equal the calculated running clearance at the possible rub location. If the relative deflection at the rub location exceeded the running clearance, a spring would be actuated to simulate the rub between the two components.

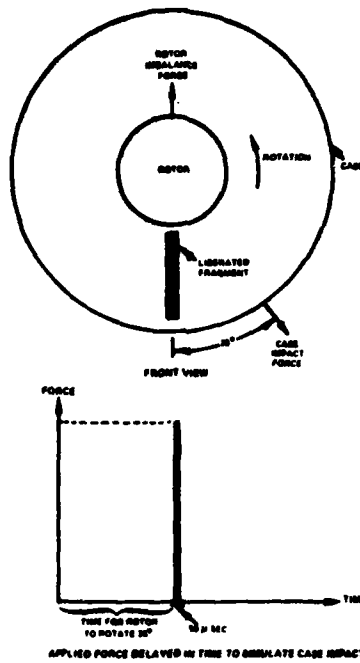


Figure 23 Rotor Transient Response – Relative Phase Between Imbalance and Impact Forces

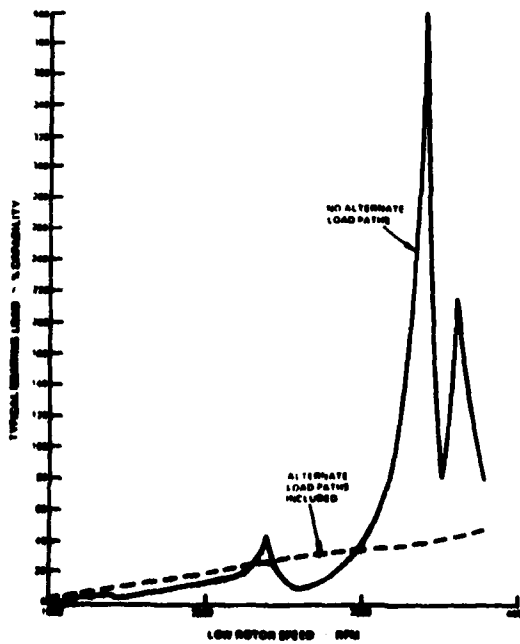


Figure 24 Rotor Transient Response – Alternate Load Paths Reduce Bearing Load

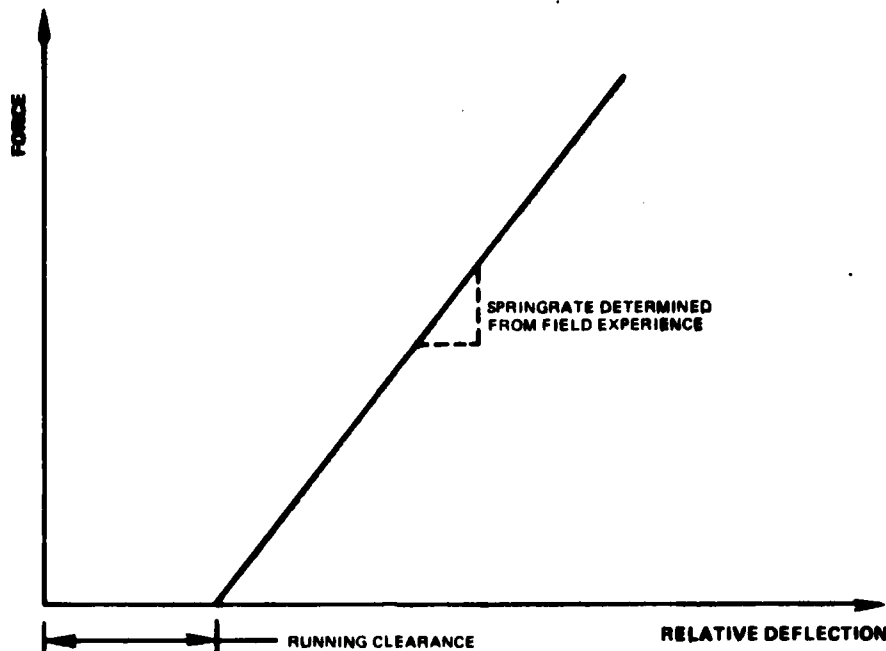


Figure 25 Rotor Transient Response – Bi-Linear Spring Used to Simulate Rub Condition

#### 4.1.5 Deceleration Response of Engine

When a rotor failure occurs near or at the maximum rotor speed, the engine must decelerate to shut down. During the deceleration, the engine may pass through several critical speeds which could produce high response loads. From the transient response analysis, the rotor reached a steady-state response condition after a short period of time. The deceleration analysis was, therefore, analyzed as a steady-state response to a rotating imbalance.

### 4.2 RESULTS OF ANALYSIS

The transient response of the entire engine as well as the deceleration steady-state response was calculated for a fan rotor failure which produced a disk fragment with energy equivalent to two and four adjacent blades and their included disk serrations. Interferences, impact and damping were included in each speed point throughout the engine operating range.

#### 4.2.1 Structural Areas of Concern

The structural component areas of concern were determined by evaluating the impact of a component failure on the engine structural integrity. Figure 26 shows the limiting engine locations for a fan rotor failure which were: engine mounts, low rotor bearings and bearing supports, fan coupling nut, low shaft, low turbine tierods, and all engine case flanges.

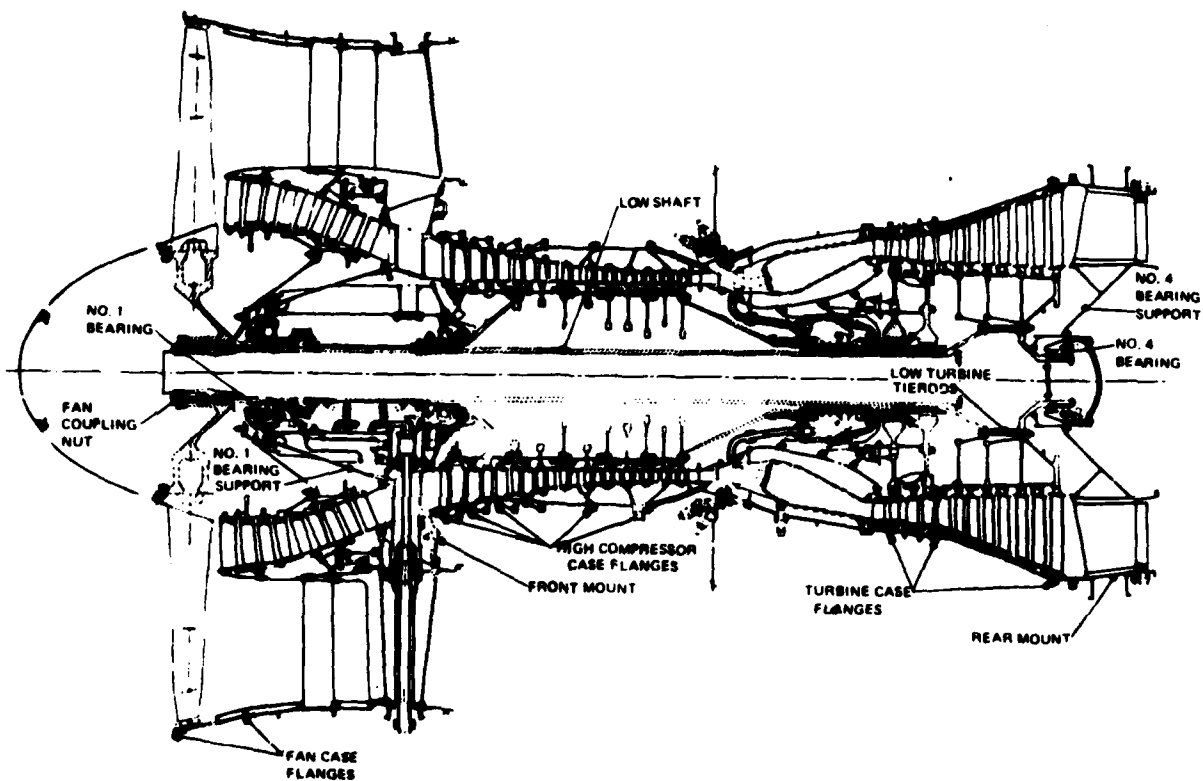


Figure 26 Engine Cross Section - Structural Areas of Concern With Loss of a Fan Disk Fragment

#### 4.2.2 Engine Component Loads

Loads for all the engine limiting locations were calculated throughout the engine operating range with the maximum transient load occurring at the maximum engine speed for all limiting locations. Figure 27 illustrates a typical deceleration response to a fan rotor failure at one limiting engine location. The maximum steady-state load was reached well down in the speed range during deceleration when the engine passed through a critical speed. However, the maximum transient load occurred at redline speed. The maximum transient loads for the limiting engine locations are summarized in Table 7. The responses for the two and four blade equivalent fan disk fragments were not linear, e.g., the response to the four blade fragment was less than twice the response to the two blade fragment. The reason for this was the bilinear springs in the system producing a response which was nonlinear with load. The impact loads were not directly additive to the rotating imbalance loads but were combined vectorally accounting for the phase angle between them.



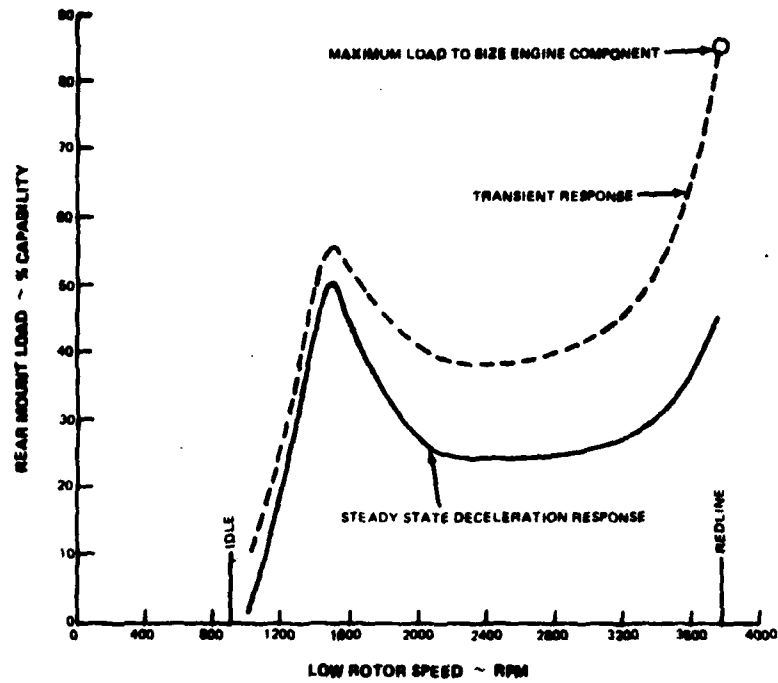


Figure 27 Typical Deceleration Response With Loss of a Fan Disk Fragment

Engine Location	Loss of Fan Disk Fragment Equivalent to Two Adjacent Fan Blades With Included Disk Serration			Loss of Fan Disk Fragment Equivalent to Four Adjacent Fan Blades With Three Included Disk Serrations		
	Rotating Load (% Capability)	Impact Load (% Capability)	Combined Load (% Capability)	Rotating Load (% Capability)	Impact Load (% Capability)	Combined Load (% Capability)
Front Mount	30	19	30	64	40	62
Rear Mount	84	13	87	136	27	137
#1 Bearing	53	21	54	70	35	72
#1 Bearing Support	66	26	66	87	44	89
#4 Bearing	27	18	32	41	30	42
#4 Bearing Support	51	33	60	77	57	80
Fan Coupling Nut	59	21	64	102	45	107
LPT Tierods	98	27	100	124	64	164
A Flange	20	6	21	31	12	33
B Flange	94	20	100	140	42	132
E Flange	67	12	66	106	23	119
F Flange	65	12	64	104	23	106
G Flange	66	12	65	103	23	106
H Flange	66	12	65	103	22	105
J Flange	68	13	70	111	21	115
K Flange	62	12	65	89	29	97
M Flange	70	13	74	117	35	117
N Flange	86	16	90	132	43	144
P Flange	82	28	85	119	55	139

Table 7 Maximum Transient Loads For the Limiting Engine Location

A typical response curve is shown in Figure 28. The total response is the sum of a forced frequency plus several natural frequencies which decay with time. The transient peak response was the load used to size the engine components.

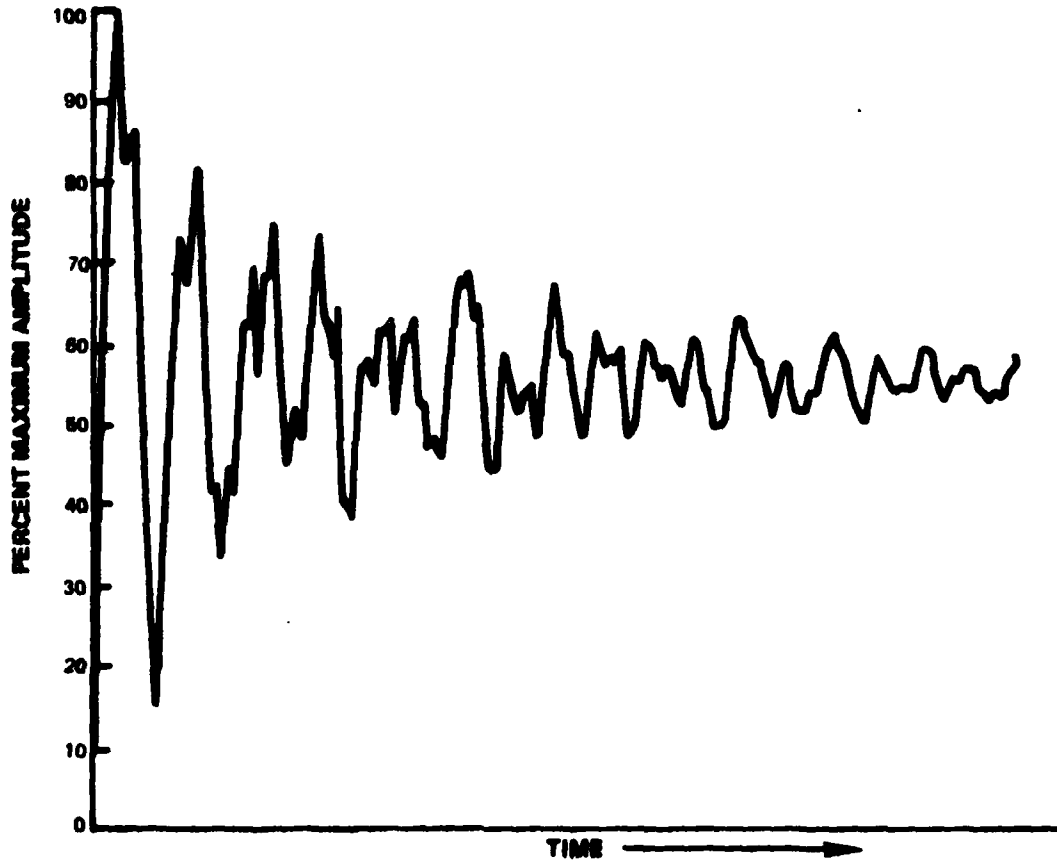


Figure 28 Typical Engine Response to Combined Rotating Imbalance and Impact Load

#### 4.2.3 Potential Solutions for Limiting Structural Components

The additional weight required for structural adequacy of the engine components is shown in Table 8. No additional weight would be required for the two blade fragment. However, 44 pounds would be required for the four blade fragment. Weight calculations were based on strengthening the present configurations to sustain the fan rotor failure loads. For some areas, such as the rear mount, a redesign of the present configuration might produce less of a weight penalty than adding material to the present configuration. However, a configuration change would require a detailed design effort which was beyond the scope of this study. As part of the study, alternate approaches to limiting the engine responses were studied.

Results of the transient response analysis indicate that limiting the rotor deflection could reduce the rotor loads. Therefore a bumper bearing on the low rotor which would limit the rotor deflection has the potential for lowering rotor loads. It would be necessary, however, to perform a trade-off study to compare the weight required for the bumper bearing vs. adding material to the low rotor.

Another alternative to limiting the engine response would be to increase the amount of damping in the engine by means of a device such as a friction damper. The friction damper, comprised of preloaded parallel plates which would break free and introduce a coulomb damping force to the system, may provide the damping necessary to control the engine response. Such a device would also require a detailed design effort and an extensive development program to evaluate and calibrate the damper before it could be incorporated into an engine. The design considerations and limitations mentioned in Section 3.1.9 are also valid with the incorporation of the aforementioned potential solutions.

<u>Component</u>	<u>Loss of Fan Disk Fragment Equivalent to Two Adjacent Fan Blades With Included Disk Serration</u>	<u>Loss of Fan Disk Fragment Equivalent to Four Adjacent Fan Blades With Three Included Disk Serrations</u>
	<u>Additional Weight (lbs.)</u>	<u>Additional Weight (lbs.)</u>
Front Mount	0	0
Rear Mount	0	7
No. 1 Bearing	0	0
No. 1 Bearing Support	0	0
No. 4 Bearing	0	0
No. 4 Bearing Support	0	0
Fan Coupling Nut	0	1
LPT Tierods	0	5
Low Shaft	0	25
Fan Case Flanges	0	1
High Compressor Case Flanges	0	1
Turbine Case Flanges	0	4
	TOTAL WEIGHT	44

**Table 8** Rotor Transient Response – Additional Weight Required For Structural Adequacy of Limiting Engine Components

## 5.0 REVIEW OF RESULTS OF THE NATIONAL AERONAUTICS AND SPACE ADMINISTRATION'S ROTOR BURST PROTECTION PROGRAM

As required under this contract, results of the National Aeronautics and Space Administration's (NASA) Rotor Burst Protection Program were to be considered in this study. This program consisted of results from spin tests conducted by the Naval Air Propulsion Test Center (NAPTC) and analytical models developed by Massachusetts Institute of Technology (MIT) to explain and understand containment devices under impact loading.

The spin tests conducted by the NAPTC\* were primarily produced by disk burst where the entire disk with and without blades separated into sectors. These sectors were typically the size of two  $180^\circ$  fragments and three  $120^\circ$  fragments. The disk fragments defined in this study were much smaller in size and lower in kinetic energy than the disk sectors (see Figure 29).

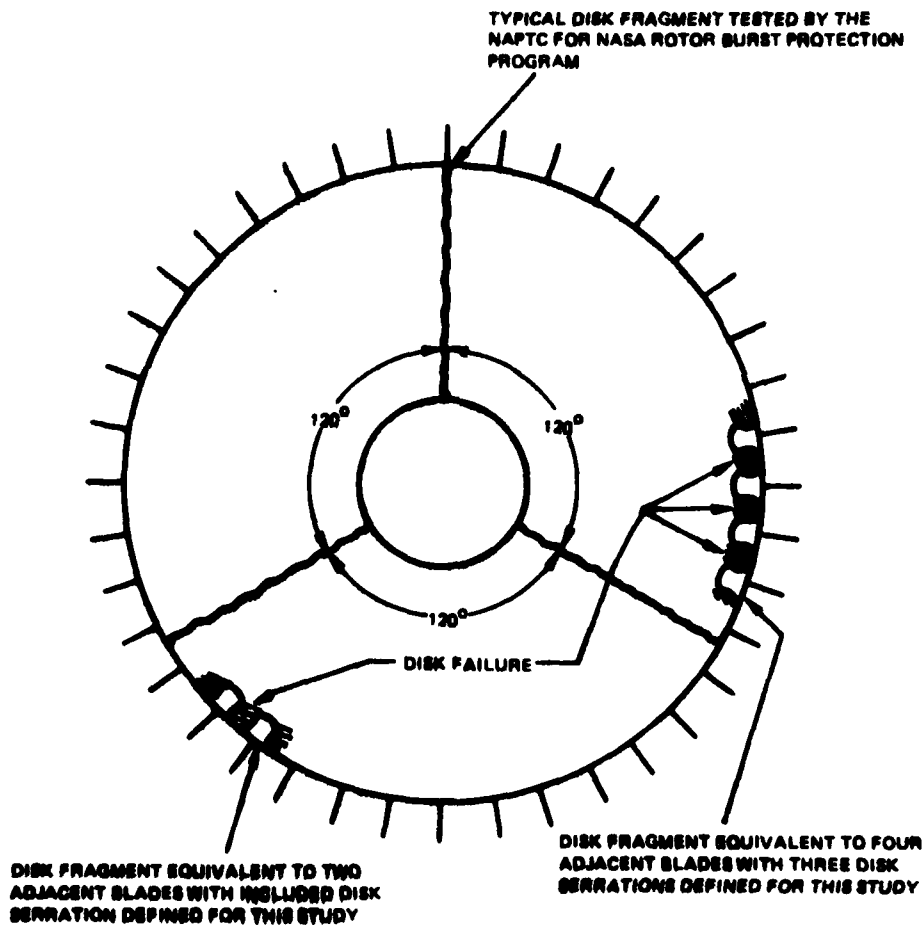


Figure 29 Comparison of Typical Disk Fragments Tested by the NAPTC and Disk Fragments Defined for This Study

\*References 2 and 3

The results of the NAPTC spin tests were not applicable to this study based on the following observations:

1. The size and kinetic energy of the disk fragments were not similar.
2. The containment case materials were not the high strength materials used in large turbine engine cases.
3. The containment cases were simply supported (not rigidly attached to a support structure) which allows greater distortion and greater energy absorption than the actual turbine engine hardware where significant radial stiffness would be provided by the adjacent material and hardware.
4. The spin tests were conducted at room temperature, so the containment cases did not experience the thermal effects on material behavior that is inherent in an operating turbine engine.

The NAPTC spin tests, however, have shown that high speed photography can be very useful in understanding the fundamental aspects of the fragment kinematics and the containment case response. A review of the MIT analytical models\* indicated that they may be very useful with further development, in the analysis and design of containment cases or devices. A main area which is missing is the development and calibration of a failure criterion to indicate when failure of the containment case or device would occur.

The containment problem could also be analyzed utilizing the nonlinear dynamic capabilities that exist in today's finite element computer programs. Two such programs are presently available at Pratt & Whitney Aircraft that could be used for a containment analysis. These tools presently lack failure criteria for containment and lack calibration with actual containment events. Both programs are finite element formulations with inelastic and transient capabilities but differ in their element selection. They both represent the state-of-the-art techniques in finite element analysis. A major problem is to define the transient loading imposed by a fragment on the containment structure.

\*References 4 thru 7

## 6.0 RESULTS

The results of this study indicated significant weight increases for the engine in order to contain the equivalent disk fragments of two blades with an included disk serration and four blades with three included disk serrations. The total resultant engine weight increases (shown in Table 9) for the two blade fragment is 367 pounds and for the four blade fragment is 682 pounds. This includes the following items:

- 210 pounds and 395 pounds for engine in-plane containment with a 10 pound and 15 pound weight reduction by substituting a titanium base alloy into the LPC. For comparison, a recent study conducted by the SAE Committee on Aircraft Engine Containment (Reference 8) showed an engine weight increase of 400 pounds for an equivalent disk fragment of three adjacent blades with two included disk serrations for similar type fan engines.
- 105 pounds for forward containment of fan blade tip fragments.
- 0 pounds and 44 pounds, for structural adequacy of engine components based on a transient response analysis.
- 52 pounds and 138 pounds to support the added engine containment material.

	<u>Disk Fragment With Energy Equivalent to Two Adjacent Blades With an Included Disk Serration</u>	<u>Disk Fragment With Energy Equivalent to Four Adjacent Blades With Three Included Disk Serrations</u>
In-Plane Containment	220 (lbs.)	410 (lbs.)
Adjustment for LPC Alternate Material (Titanium Base Alloy)	-10	-15
Sub Total	210	395
Additional Weight to Support the Added Containment Material	(25%) 52	(35%) 138
Forward Containment (Fan Blade Tip Fragments)	105	105
Structural Adequacy of Engine Components Based on Transient Response Analysis	0	44
Total	367 (lbs.)	682 (lbs.)

*Table 9 Total Resultant Engine Weight Increase*

**The support material outside the radial plane of the rotor stage is required because:**

- 1) Engine case thermal stresses and resulting safe operating lives would be affected because of the thermal gradients produced between the very thin to thick cross-sections in the case.**
- 2) Case bolting and other hardware would have to be modified in order to carry the increase in impact load.**

**As mentioned in Section 3.1.9, this additional weight will have an effect on other engine design considerations and limitations as given below:**

- 1) Engine seal clearances would change because of changes in the thermal response of the engine cases. The thick cases would have a slower growth response and cause the blade tips to rub, thus opening the blade tip clearance. The engine performance and surge margins would therefore be significantly affected.**
- 2) Case natural frequencies would change due to the added weight plus all case responses to engine excitations (example, blade passing frequency) would have to be rechecked.**
- 3) Engine assembly would become more complex due to changes required in plumbing, bolting and handling the heavier cases.**
- 4) Ultimate increase in cost to the consumer would result because of the increase in weight and fundamental performance disadvantage of thick engine cases.**

**A transient response analysis performed on the engine, that included the additional containment weight, would be expected to be similar to the current analysis. The majority of the additional weight would be in the case structure, with the rotor and supports remaining relatively unchanged with little change in the rotor.**

**The JT9D-59A/70A engine was found to be relatively insensitive to large imbalance at the fan location created by the liberated fragments. Blade tip rubs provided additional supports to the rotor thereby limiting the rotor excursion. The relative insensitivity of the engine had been previously exhibited in the single fan blade field failures experience to date in similar engine models.**

**The additional weight will have a serious effect on the basic engine integrity. Such effects as the evaluation of the structural integrity due to the induced thermal stresses and the effect on the engine performance were beyond the scope of this study.**

## **GLOSSARY**

**Aft Containment** – Containment required rearward of the fan rotor plane

**Blade Passing Frequency** – Frequency at which the blades pass a stationary point equal to the number of blades times the rotor speed

**Bore Fracture Mechanics** – A common technique, modified to eliminate disk-bore fracture

**Critical Speed** – Natural frequency of the engine which is capable of being excited by rotor imbalance

**Disk Serration** – Integral disk material which mates with a blade dovetail

**Dovetail** – The portion of a blade which mates with a disk serration

**Fan Exit Guide Vanes** – Vanes provided downstream of the fan to straighten the fan duct air flow

**Fan Splitter** – Device which separates the fan duct air flow from the engine core air flow

**Forward Containment** – Containment required forward of the fan rotor plane

**Heat of Material** – A quantity of material heat treated at the same time

**Imbalance** – Offset of the rotor mass center caused by a liberated fragment

**One Pitch Length** – Case circumference divided by the number of blades in the rotor stage

**Redline** – Maximum engine operating speed

**Rotor/Frame** – An entire engine rotor with bearings, bearing supports, cases, and mounts

**Shear Plug** – Piece of material punched out from a containment case with a perimeter of the impacting fragment and the thickness of the containment case

**Surge Margin** – Percent of pressure ratio above the operating line at which engine surge would occur

**Ultrasonic Inspection** – Inspection technique using high frequency sound waves



## REFERENCES

1. Dennis, A.J., Eriksson, R.H., Seitelman, L.H., "Transient Response Analysis of Damped Rotor Systems by the Normal Mode Method," A.S.M.E. Publication 75-GT-58, March 2, 1975.
2. Mangano, G.J., "Rotor Burst Protection Program, Phases VI and VII: Exploratory Experimentation to Provide Data for the Design of Rotor Burst Fragment Control Rings," NAPTC-AED-1968, March 1972.
3. Mangano, G.J., Salvino, J.F., and DeLucia, R.A., "Rotor Burst Protection Program: Experimentation to Provide Guidelines for the Design of Turbine Rotor Burst Fragment Containment Rings," NAPTC-PE-98, NASA-CR-135166, March 1977.
4. McCallum, R.B., Leech, J.W., and Witmer, E.A., "Progress in the Analysis of Jet Engine Burst-Rotor Containment Devices," ASRL TR 154-1, August 1969.
5. Wu, R. W-H., and Witmer, E.A., "Finite-Element Analysis of Large Transient Elastic-Plastic Deformations of Simple Structures, with Application to the Engine Rotor Fragment Containment/Deflection Problem," ASRL TR 154-4, NASA CR-120886, January 1972.
6. Wu, R. W-H., and Witmer, E.A., "Computer Program - Jet 3 - to Calculate the Large Elastic-Plastic Dynamically-Induced Deformations of Free and Restrained, Partial and/or Complete Structural Rings," ASRL TR 154-7, NASA CR-120993, August 1972.
7. Stagliano, T.R., Spilker, R.L., Witmer, E.A., "User's Guide to Computer Program CIVM-JET 4B to Calculate the Transient Structural Responses of Partial and/or Complete Structural Rings to Engine-Rotor-Fragment Impact," ASRL TR 154-9, NASA CR-134907, March 1976.
8. Report of S.A.E. Committee on Aircraft Engine Containment, (to be published).